ORIGINAL ARTICLE

# Phase I dose-finding and pharmacokinetic study of the oral epidermal growth factor receptor tyrosine kinase inhibitor Ro50-8231 (erlotinib) in Japanese patients with solid tumors

Noboru Yamamoto · Atsushi Horiike · Yasuhito Fujisaka · Haruyasu Murakami ·
Tatsu Shimoyama · Yasuhide Yamada · Tomohide Tamura

## Abstract

*Purpose* The objectives of this phase I dose-finding study of erlotinib were to investigate the toxicity profile, to confirm the acceptable toxicity of doses up to 150 mg/day, and to assess the pharmacokinetic (PK) profile and antitumor activity in Japanese patients with solid tumors.

*Patients and methods* Patients with solid tumors not amenable to standard forms of treatment were included. Treatment cycle 1 consisted of single-dose administration on day 1, withdrawal on day 2, continuous daily administration from days 3–23, and withdrawal from days 24–30. Subsequent cycles (28 days) used continuous daily administration. The dose of erlotinib was escalated from 50 mg/day to 150 mg/day in 50-mg increments. PK evaluation was performed in all patients during cycle 1.

*Results* Fifteen patients, aged 38–70 (median; 57) years with non-small-cell lung (n = 11), colorectal (n = 3) or head and neck (n = 1) cancer were enrolled. The major toxicities were rash, diarrhea and liver dysfunctions, which were generally mild and easily manageable. The good tolerability of erlotinib up to the dose of 150 mg/day was confirmed. One patient developed grade 5 treatment-related interstitial pneumonitis. Four of 11 evaluable patients achieved partial responses; all four had non-small-cell lung cancer (NSCLC). The peak plasma concentration of erlotinib, and the area under the concentration-time curve increased proportionally to the dose, suggesting linear PK.

*Conclusion* The recommended dose of erlotinib in Japanese patients is 150 mg/day. Further trials in Japanese NSCLC patients are warranted.

**Keywords** Phase I study · EGFR · Tyrosine kinase inhibitor · Ro50-8231 · Erlotinib · Tarceva

N. Yamamoto · A. Horiike · Y. Fujisaka · H. Murakami ·
T. Shimoyama · Y. Yamada · T. Tamura (✉)
Division of Internal Medicine, National Cancer Center Hospital,
5-1-1, Tsukiji Chuo-ku, Tokyo 104-0045, Japan
e-mail: ttamura@ncc.go.jp

## Introduction

The epidermal growth factor receptor (EGFR) is a transmembrane receptor that has been shown to play an important role in the growth and survival of many solid tumors. Ligand-activated EGFR-dependent signaling is involved in cell proliferation, apoptosis, angiogenesis, invasion, and metastasis [5, 12, 21, 26]. Targeting EGFR has already been recognized as a promising molecular approach in cancer therapy.

Ro50-8231 (erlotinib, Tarceva®) is an orally available, quinazoline-based, highly selective, reversible inhibitor of EGFR tyrosine-kinase activity. This agent competes with adenosine triphosphate for binding to the intracellular tyrosine-kinase domain of EGFR, thus inhibiting receptor phosphorylation. In preclinical studies, the 50% inhibitory concentration of erlotinib was 2 nM, and substantial antitumor activity was demonstrated against human colorectal, head and neck, non-small-cell lung, and pancreatic tumor cells [1, 4, 9]. Following promising preclinical studies, erlotinib was investigated in 40 patients with advanced solid tumors [10]. In this initial US-based phase I study, the major toxicities with once-daily erlotinib were diarrhea, rash, mucositis, headache, and hyperbilirubinemia. The incidence and severity of diarrhea and skin rash were related to the dose of erlotinib and determined as dose-limiting toxicities (DLTs). DLTs were noted at 200 mg/day and, therefore,

150 mg/day was selected as the recommended dose for further studies [10].

Based on the results of the initial US phase I study, we conducted a phase I study of erlotinib in Japanese patients with solid tumors. The objectives of this study were (1) to assess the toxicity profile of erlotinib, including DLTs, (2) to confirm the acceptable tolerability of erlotinib up to a dose of 150 mg/day, (3) to assess the pharmacokinetic (PK) profile of erlotinib, and (4) to assess antitumor activity.

## Patients and methods

### Patient eligibility

Patients were eligible if they had histologically or cytologically confirmed malignant solid tumors that were resistant to standard therapies, or for which there was no effective treatment. The tumor types selected were among those known to commonly overexpress EGFR, but patients were not selected on the basis of individual EGFR status. Eligibility criteria also included the following: age 20–74 years; Eastern Cooperative Oncology Group (ECOG) performance status (PS) 0–2; life expectancy greater than 3 months; no previous chemotherapy, radiation therapy, or surgery within 4 weeks before treatment with erlotinib (6 weeks for previous treatment with nitrosoureas or mitomycin); adequate bone marrow, hepatic and pulmonary functions (absolute neutrophil count $\geq$ 1,500/mm$^3$, platelet count $\geq$ 100,000/mm$^3$, hemoglobin $\geq$ 9.0 g/dl, total serum bilirubin $\leq$ 1.5 mg/dl, aspartate aminotransferase [AST] $\leq$ 100 IU/l, alanine aminotransferase [ALT] $\leq$ 100 IU/l, serum creatinine $\leq$ 1.5 mg/dl, arterial oxygen pressure [PaO$_2$] $\geq$ 70 torr). Exclusion criteria included: pregnancy or lactation; symptomatic brain metastasis; previous treatment with other EGFR tyrosine-kinase inhibitors or trastuzumab; a history of hypersensitivity reactions to any drugs; pleural effusion and ascites that required drainage; malabsorption syndrome or any other disorder that would affect gastrointestinal absorption; hepatic B or C virus or human immunodeficiency virus infection; serious pre-existing medical conditions such as uncontrolled infections, severe heart disease, uncontrolled diabetes and psychogenic disorders; concomitant use of a contact lens or active corneal disease.

Written informed consent was obtained from all patients. This study was approved by the institutional review board at the National Cancer Center, and conducted in accordance with Japanese Good Clinical Practice guidelines.

### Drug administration

Erlotinib was supplied by Chugai Pharmaceutical Co. Ltd. (Tokyo, Japan) as 25, 100 and 150 mg tablets. The agent was administered orally with 200 ml of water in the morning, 1 h before breakfast. Subjects fasted for at least 2 h before and 1 h after administration. The initial treatment cycle consisted of single dose administration on day 1, withdrawal on day 2, continuous daily administration from day 3 to day 23 (21 days), and withdrawal from day 24 to day 30 (7 days). Both withdrawal periods were planned for PK assessment. From the second cycle onwards, erlotinib was administered daily without intervals. Cycles were repeated every 4 weeks (Fig. 1).

### Dose escalation procedure

Based on the results of the previously reported US study [10], the starting dose of erlotinib was determined as 50 mg, escalating in 50 mg increments up to 150 mg. Three patients were entered at the initial dose level. If dose limiting toxicity (DLT) was observed in one-third of the patients at this dose level, an additional three patients were entered at the same dose level. Six patients were entered at the second (100 mg) and third (150 mg) dose levels. The dose level at which at least two patients experienced DLTs was defined as the maximum tolerated dose (MTD). The definition of DLT was as follows: (1) grade 3/4 hematologic toxicity, (2) grade 3/4 non-hematologic toxicity excluding skin toxicity, AST/ALT elevation and hyperbilirubinemia, (3) grade 4 skin toxicity, (4) grade 4 AST/ALT elevation or grade 3 AST/ALT elevation lasting more than 7 days, (5) hyperbilirubinemia (>3.5 mg/dl or 2.5–3.5 mg/dl lasting more than 7 days).

### Pretreatment assessment and follow-up studies

Complete clinical assessments, including physical examination, ECOG PS, blood pressure, weight, electrocardiogram, chest X-ray, and routine laboratory tests were evaluated in all patients before study entry and prior to each subsequent treatment cycle. Routine laboratory tests included a complete blood count and differential testing of electrolytes, total serum protein, albumin, total serum bilirubin, AST, ALT, alkaline phosphatase, lactic dehydrogenase, gamma-glutamyl transferase, serum creatinine, uric
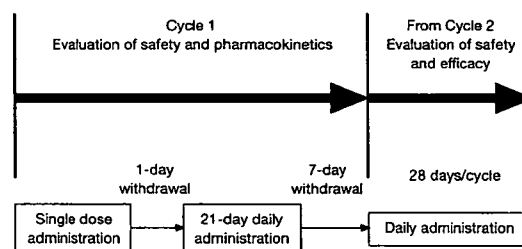


**Fig. 1** Treatment schema

acid, cholesterol, glucose, $PaO_2$, adequate tumor markers and urinalysis. With the exception of $PaO_2$, tumor markers and urinalysis, these laboratory tests were repeated on days 1, 3, 10, 17, 24 and 31, and then weekly. $PaO_2$ was obtained as occasion demanded. Tumor markers and urinalysis were determined before each treatment cycle and biweekly, respectively. Toxicities were evaluated according to the National Cancer Institute common toxicity criteria (NCI-CTC, version 2.0). Tumor responses were evaluated according to RECIST (response evaluation criteria in solid tumors) criteria [23].

## Pharmacokinetics

PK evaluation was performed in all patients during the initial cycle of treatment. Heparinized venous blood samples (5 ml) were taken: before treatment and 1, 2, 4, 6, 8, 10, 24, 34 and 48 h after treatment on day 1; before treatment on days 4, 10, and 17; before treatment on the last treatment day (day 23) of cycle 1, and 1, 2, 4, 6, 8, 10, 24, 34 and 48 h after this treatment administration. Blood samples were immediately centrifuged at 1,500 rpm for 10 min, and plasma was aliquoted and stored at $\leq -70°C$ in polyethylene tubes until analysis. The plasma concentrations of erlotinib and its O-desmethylated metabolite (OSI-420) were measured by reverse-phase high-performance liquid chromatography using ultraviolet absorbance detection, as described previously [14].

Individual plasma erlotinib and OSI-420 concentration data were analyzed by non-compartmental methods analysis using the WINNonlin software program version 1.5 (Pharsight Corporation, CA, USA). Derived PK parameters included the maximum plasma drug concentration ($C_{max}$), time to $C_{max}$ ($t_{max}$), area under the plasma drug concentration-time curve from 0 to 24 h ($AUC_{0-24}$) and to infinity ($AUC_{0-inf}$), terminal half-life ($t_{1/2}$) and the oral clearance ($Cl/F$). To assess the drug accumulation by daily administration, the accumulation index ($R$) was calculated according to the following formula: $R = 1/(1 - \exp^{-Ke t})$, where Ke is the elimination rate constant and $t$ is the administration interval.

## Results

### Patient characteristics

Fifteen patients were enrolled between April 2002 and October 2002. Patient characteristics are listed in Table 1. There were 11 males and four females with a median age of 57 (range, 38–70) years. The predominant tumor type was non-small-cell lung cancer (NSCLC). A total of 78 cycles (28 days/cycle) of erlotinib were administered, and the

**Table 1** Patient characteristics

| Characteristic | | No. of patients |
|---|---|---|
| Total no. of patients | | 15 |
| Male/female | | 11/4 |
| Age (years); median (range) | | |
| Median | 57 | |
| Range | 38–70 | |
| ECOG performance status | | |
| 0 | | 3 |
| 1 | | 12 |
| Tumor type | | |
| NSCLC | | 11 |
| Colorectal | | 3 |
| Head and neck | | 1 |
| Prior treatment | | |
| Surgery | | 5 |
| Radiotherapy | | 4 |
| Chemotherapy | | 14 |
| No. of prior chemotherapy regimens | | |
| 0 | | 1 |
| 1 | | 8 |
| 2 | | 3 |
| 3 | | 2 |
| 4 | | 1 |

*NSCLC* non-small-cell lung cancer

median number of cycles administered per patient was three (range, 1–19). All 15 patients were included in the toxicity evaluation, and 11 patients were evaluable for efficacy according to the RECIST criteria. Of the four patients not evaluable (NE) for efficacy, one was excluded due to interstitial lung disease (ILD). This patient received erlotinib 100 mg/day, and was withdrawn from the study due to the development of interstitial pneumonitis after 8 days of treatment during cycle 1. Of the remaining three patients, one was regarded as NE because the previously documented brain metastasis was not scanned during the screening period (even though the evaluable supraclavicular lymph node metastasis remained stable through seven cycles of treatment). The other two patients chose to stop treatment. Their target lesions had progressed by about 6–15% after the first cycle of treatment, but their tumor responses met neither SD nor PD according to RECIST criteria, and therefore were classed as NE.

### Toxicity

The major toxicities in the first cycle and in all cycles combined are listed in Tables 2 and 3, respectively. Rash and diarrhea were the principal toxicities associated with

**Table 2** Major toxicities in the first cycle

| Erlotinib dose (mg/day) | 50 | | | 100 | | | 150 | | | All | | | Total | % |
|---|---|---|---|---|---|---|---|---|---|---|---|---|---|---|
| No. of patients | 3 | | | 6 | | | 6 | | | 15 | | | | |
| NCI-CTC grade | 1 | 2 | ≥3 | 1 | 2 | ≥3 | 1 | 2 | ≥3 | 1 | 2 | ≥3 | | |
| Leukopenia | 1 | 0 | 0 | 0 | 0 | 0 | 0 | 0 | 0 | 1 | 0 | 0 | 1 | 6.7 |
| Neutropenia | 0 | 0 | 0 | 2 | 0 | 0 | 0 | 0 | 0 | 2 | 0 | 0 | 2 | 13.3 |
| Anemia | 1 | 0 | 0 | 0 | 0 | 0 | 1 | 1 | 0 | 2 | 1 | 0 | 3 | 20.0 |
| Skin rash | 1 | 1 | 0 | 4 | 1 | 0 | 1 | 5 | 0 | 6 | 7 | 0 | 13 | 86.7 |
| Diarrhea | 1 | 0 | 0 | 2 | 0 | 0 | 5 | 0 | 0 | 8 | 0 | 0 | 8 | 53.3 |
| Stomatitis | 0 | 0 | 0 | 1 | 0 | 0 | 2 | 1 | 0 | 3 | 1 | 0 | 4 | 26.7 |
| Keratitis | 0 | 0 | 0 | 1 | 0 | 0 | 1 | 0 | 0 | 2 | 0 | 0 | 2 | 13.3 |
| Pneumonitis | 0 | 0 | 0 | 0 | 0 | 1* | 0 | 0 | 0 | 0 | 0 | 1* | 1 | 6.7 |

* Grade 5

**Table 3** Major toxicities in all cycles

| Erlotinib dose (mg/day) | 50 | | | 100 | | | 150 | | | All | | | Total | % |
|---|---|---|---|---|---|---|---|---|---|---|---|---|---|---|
| No. of patients | 3 | | | 6 | | | 6 | | | 15 | | | | |
| NCI-CTC grade | 1 | 2 | ≥3 | 1 | 2 | ≥3 | 1 | 2 | ≥3 | 1 | 2 | ≥3 | | |
| Leukopenia | 1 | 0 | 0 | 2 | 0 | 0 | 1 | 0 | 0 | 4 | 0 | 0 | 4 | 26.7 |
| Neutropenia | 0 | 0 | 0 | 3 | 0 | 0 | 0 | 0 | 0 | 3 | 0 | 0 | 3 | 20.0 |
| Anemia | 1 | 0 | 0 | 2 | 0 | 0 | 3 | 1 | 0 | 6 | 1 | 0 | 7 | 46.7 |
| Skin rash | 1 | 1 | 0 | 4 | 1 | 0 | 1 | 5 | 0 | 6 | 7 | 0 | 13 | 86.7 |
| Diarrhea | 2 | 0 | 0 | 4 | 0 | 0 | 4 | 1 | 0 | 10 | 1 | 0 | 11 | 73.3 |
| Stomatitis | 0 | 0 | 0 | 2 | 0 | 0 | 2 | 1 | 0 | 4 | 1 | 0 | 5 | 33.3 |
| Keratitis | 0 | 0 | 0 | 3 | 0 | 0 | 2 | 0 | 0 | 5 | 0 | 0 | 5 | 33.3 |
| ALT increased | 1 | 0 | 0 | 3 | 2 | 0 | 3 | 2 | 0 | 7 | 4 | 0 | 11 | 73.3 |
| AST increased | 2 | 0 | 0 | 3 | 1 | 0 | 3 | 0 | 0 | 8 | 1 | 0 | 9 | 60.0 |
| Total protein decreased | 1 | 0 | 0 | 4 | 0 | 0 | 3 | 0 | 0 | 8 | 0 | 0 | 8 | 53.3 |
| Pneumonitis | 0 | 0 | 0 | 0 | 0 | 1* | 0 | 0 | 0 | 0 | 0 | 1* | 1 | 6.7 |

ALT alanine aminotransferase, AST aspartate aminotransferase

* Grade 5

erlotinib. Hematologic toxicities were generally mild (grade 1–2) in severity.

Rash was experienced by 13 (86.7%) of 15 assessable patients, and mostly consisted of rash and seborrhea. The onset of these skin toxicities generally occurred between days 10–14 of cycle 1, and persisted with continued erlotinib treatment. The rash was less than or equal to grade 2 in severity and almost asymptomatic. Supportive treatment with various dermatologic medications, including riboflavin, vitamin B6 and minocyclin did not resolve or relieve these skin effects, although they were clinically tolerable. Although the skin manifestations were qualitatively similar in all affected patients, they occured more frequently with the higher doses of erlotinib.

🙋 Springer

Diarrhea was observed in 11 (73.3%) of 15 patients (Table 3). The onset of diarrhea generally occurred during the initial treatment cycle. This toxicity was generally mild (grade 1–2) in severity, and watery diarrhea was not observed. The diarrhea was generally manageable, and responded to treatment with a lactobacillus preparation; loperamide was not required.

ALT and AST elevations, were observed in 11 (73.3%) and 9 (60.0%) of 15 patients (Table 3), respectively. However, these toxicities were mild (grade 1–2) in severity, and improved without any medication during treatment with erlotinib. Stomatitis and keratitis, including corneal erosion, were generally mild, and did not seem to be dose-related.

Grade 5 pulmonary toxicity was observed in one patient at the 100 mg/day dose level. The patient was a 68-year-old male with PS 1, who was diagnosed with advanced NSCLC, and had previously suffered from tuberculosis and had chronic emphysema. Before study entry, this patient had received 5 cycles of first-line cisplatin and irinotecan chemotherapy. He complained of dyspnea, and a chest X-ray and computed tomography scan on the eighth day of erlotinib treatment showed a ground-glass appearance in the left lung, suggestive of interstitial pneumonitis. The bronchoalveolar lavage fluid did not suggest the presence of any infections such as fungus, *Pneumocystis carinii,*. Neither steroid hormone (60 mg/day of predonisolone) nor pulse steroid therapy (1,000 mg/day of methylprednisolone for 3 days) improved his pulmonary condition, and he died on day 34 of treatment. An autopsy was performed and the pathologic findings demonstrated severe emphysematous changes, with alveolar destruction and pyogenic bronchopneumonia with infiltration of inflammatory cells, as well as disease progression. Although the pathological findings did not support drug-induced interstitial pneumonitis, the clinical observations indicated suspected drug- induced interstitial pneumonitis that could have exacerbated respiratory failure.

Up to a dose level of 150 mg/day, one DLT was observed (grade 5 pulmonary toxicity at a dose of 100 mg/day); other toxicities were considered acceptable. Therefore, the MTD was not reached, and the acceptable tolerability of erlotinib doses up to 150 mg/day was confirmed. The dose level of erlotinib 150 mg/day was, therefore, determined as the recommended dose.

Antitumor activity

Eleven of 15 patients were evaluable for anti-tumor response (Table 4). Four patients (all NSCLC) achieved a partial response and three achieved stable disease (all NSCLC). Of the four responders, three were male former smokers (>50 pack years) and one was a female never-smoker; all had tumours with adenocarcinoma histology.

**Table 4** Objective tumor response and duration

| No. | Dose level (mg/day) | Age | Sex | PS | Smoking status | Tumor type | Histology | Response | Response duration (days) |
|---|---|---|---|---|---|---|---|---|---|
| 01 | 50 | 56 | M | 1 | Smoker[a] | NSCLC | Large-cell carcinoma | NE | |
| 02 | 50 | 52 | M | 1 | Smoker[a] | NSCLC | Adenocarcinoma | PD | |
| 03 | 50 | 60 | F | 1 | Never smoker | Colorectal | Adenocarcinoma | PD | |
| 04 | 100 | 62 | M | 1 | Smoker[a] | NSCLC | Adenocarcinoma | PR | 85 |
| 05 | 100 | 57 | M | 1 | Smoker[a] | NSCLC | Adenocarcinoma | SD | 87 |
| 06 | 100 | 38 | M | 1 | Smoker[a] | NSCLC | Adenocarcinoma | NE | |
| 07 | 100 | 68 | M | 1 | Smoker[a] | NSCLC | Undifferentiated | NE | |
| 08 | 100 | 50 | F | 1 | Never smoker | NSCLC | Adenocarcinoma | PR | >283[b] |
| 09 | 100 | 60 | F | 0 | Never smoker | NSCLC | Adenocarcinoma | SD | 197 |
| 10 | 150 | 48 | M | 1 | Smoker[a] | Colorectal | Adenocarcinoma | NE | |
| 11 | 150 | 53 | M | 0 | Smoker[a] | NSCLC | Undifferentiated | SD | >170[b] |
| 12 | 150 | 70 | M | 1 | Smoker[a] | NSCLC | Adenocarcinoma | PR | >170[b] |
| 13 | 150 | 53 | F | 0 | Smoker[a] | Colorectal | Adenocarcinoma | PD | |
| 14 | 150 | 58 | M | 1 | Smoker[a] | Head and Neck | Adenocarcinoma | PD | |
| 15 | 150 | 58 | M | 1 | Smoker[a] | NSCLC | Adenocarcinoma | PR | >170[b] |

*M* male, *F* female, *PS* performance status, *NSCLC* non-small-cell lung cancer, *PR* partial response, *SD* stable disease, *PD* progressive disease, *NE* not evaluable

[a] Former smoker

[b] shifted to the continuous administration study from phase I portion of trial ($n = 4$)

## Pharmacokinetics

Plasma sampling for PK analyses was performed in all 15 patients on days 1 and 4. However, plasma sampling on days 10, 17 and 23 was not undertaken in one patient due to withdrawal following pulmonary toxicity.

The PK profile of erlotinib is summarized in Table 5, and the mean plasma concentration-time profiles of erlotinib and its principal metabolite OSI-420, after treatment with erlotinib 150 mg/day are illustrated in Fig. 2. Following oral ingestion of erlotinib on day 1, mean $T_{max}$ was 6.00 h (range, 1–24 h), with a long plasma half-life ($t_{1/2}$; mean 25.92 h, range 14.84–40.02). The Cl/$F$ of erlotinib showed moderate inter-individual variability and the mean ± standard deviation (SD) [CV%] of Cl/$F$ on day 1 for erlotinib doses of 50, 100 and 150 mg/day were 12.23 ± 9.03 [73.8%], 8.84 ± 4.48 [50.7%] and 5.42 ± 1.58 [29.2%] l/h, respectively. Steady-state plasma concentrations of erlotinib were achieved by day 10 at all doses. Both $C_{max}$ and $AUC_{0-inf}$ on day 1 generally increased with erlotinib dose, suggesting linear PK in the range 50–150 mg/day (Fig. 3). The estimated and observed accumulation indexes, which were termed "$R_{est}$" and "$R_{obs}(AUC_{0-24})$", were 1.70 ± 0.61 and 2.01 ± 1.27 (mean ± SD) at the dose of 100 mg/day, respectively, and 2.12 ± 0.55 and 3.71 ± 2.40 at the dose of 150 mg/day, respectively.

OSI-420 could be reliably measured even when erlotinib was administered at a dose of 50 mg/day. When erlotinib was given at 150 mg/day on day 1, mean $T_{max}$ was 9.7 h

(range, 1–24 h), and the mean ± SD values of $C_{max}$ and $AUC_{0-24}$ were 62.7 ± 41.4 ng/ml and 789.6 ± 300.8 ng hr/ml, respectively. Exposure to OSI-420 relative to that of erlotinib was low, and the mean ± SD values for the ratio of OSI-420 $AUC_{0-24}$ to erlotinib $AUC_{0-24}$ on days 1 and 23 were 0.055 ± 0.006 and 0.074 ± 0.025, respectively. Although there was a small number of patients in this phase I study, rash seemed to be correlated with $C_{max}$ and $AUC_{0-inf}$ of erlotinib (Fig. 4).

## Discussion

Here we report a phase I dose-finding study of the oral EGFR tyrosine-kinase inhibitor erlotinib, administered daily to Japanese patients with solid tumors. In a previous, US-based phase I study, the MTD of erlotinib was determined as 150 mg/day, and this was established as the recommended dose [10]. Based on the results of this earlier study, dose escalation in the present study was limited to the assessment of erlotinib doses up to 150 mg/day (50, 100 and 150 mg/day). Only one DLT (grade 5 pulmonary toxicity) was observed in this study and the major toxicities were rash, diarrhea and elevated hepatic transaminases. At doses of erlotinib up to 150 mg/day, these toxicities were generally mild in severity, and treatment interruption was not required. Furthermore, severe haematological toxicity associated with conventional chemotherapy (such as febrile neutropenia or anemia requiring blood transfusions) was

**Table 5** Pharmacokinetic parameters of erlotinib

| Dose level (mg/day) | Day | No. of patients | $C_{max}$ (ng/ml) | $T_{max}$ (h) | Cl/F (l/h) | $t_{1/2}$ (h) | Css, min (ng/ml) | $AUC_{0-24}$ (ng hr/ml) | $AUC_{0-inf}$ (ng hr/ml) | $R_{est}$ | $R_{obs}$ ($AUC_{0-24}$) |
|---|---|---|---|---|---|---|---|---|---|---|---|
| 50 | 1 | 3 | 193.67 ± 84.39 | 5.00 ± 3.61 | 12.23 ± 9.03 | 14.76 ± 10.51 | | 3265.82 ± 1777.92 | 6320.86 ± 5015.47 | | |
| | 23 | 3 | 820.33 ± 347.25 | 4.33 ± 4.93 | 3.92 ± 2.36 | 23.60 ± 15.83 | 538.67 ± 286.49 | 15843.67 ± 7991.56 | 37798.87 ± 29387.24 | 1.51 ± 0.54 | 4.89 ± 0.58 |
| 100 | 1 | 6 | 570.67 ± 266.97 | 6.00 ± 9.01 | 8.84 ± 4.48 | 17.98 ± 11.06 | | 7704.90 ± 3550.83 | 14095.46 ± 7194.74 | | |
| | 23 | 5 | 1023.40 ± 320.15 | 3.00 ± 2.00 | 10.03 ± 8.95 | 15.56 ± 8.66 | 453.00 ± 380.27 | 14622.61 ± 7007.19 | 25616.14 ± 15011.00 | 1.70 ± 0.61 | 2.01 ± 1.27 |
| 150 | 1 | 6 | 958.00 ± 457.19 | 6.00 ± 8.92 | 5.42 ± 1.58 | 25.92 ± 9.31 | | 12845.48 ± 3774.53 | 29473.52 ± 7569.01 | | |
| | 23 | 6 | 2384.33 ± 932.43 | 1.83 ± 0.41 | 5.08 ± 4.51 | 27.19 ± 9.07 | 1642.00 ± 1085.15 | 42678.50 ± 20434.75 | 107751.87 ± 73129.00 | 2.12 ± 0.55 | 3.71 ± 2.40 |

Data represent mean ± SD

Cl/F (day 1), Dose/$AUC_{0-inf}$ (day 1), Dose/$AUC_{0-24}$ (day 23), Dose/$AUC_{0-24}$, F bioavailability, Inf infinity, $R_{est}$ estimated accumulation index, $R_{obs}$($AUC_{0-24}$) observed accumulation index of $AUC_{0-24}$ on day 23
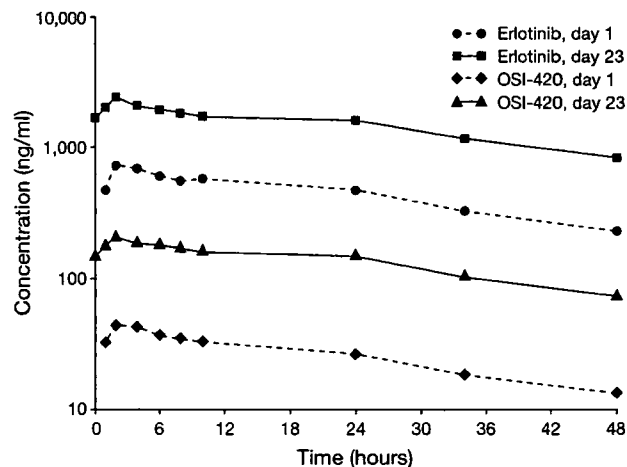


**Fig. 2** Mean plasma concentration–time profiles of erlotinib and OSI-420 following administration of erlotinib 150 mg

not observed. Therefore a dose of erlotinib 150 mg/day was determined as the recommended dose for further study in Japanese patients. The major toxicities observed in this study have also been reported for other EGFR inhibitors [2, 3, 15]. Exposure to erlotinib appears to be an important factor for the onset of certain toxicities. In the US phase I study of erlotinib, the incidence and severity of rash and diarrhea were related to the dose of erlotinib [10]. Although there was a limited number of patients and dose escalation was not planned above the dose of 150 mg/day, PK analyses in the present study also suggested a correlation between rash and drug exposure (e.g. $C_{max}$ and AUC). Other PK analyses performed in this study showed that although there was moderate inter-individual variability, linear PK profiles were observed in the range of erlotinib 50–150 mg/day, and there was no significant drug accumulation. In addition, several PK findings concerning the influence of smoking have been reported [6, 8]. Smoking could cause induction of the CYP1A2 enzyme which plays an important role in erlotinib metabolism. Although this effect could reduce the AUC of erlotinib, the effect of enzyme induction could be expected to last for only 1–2 weeks after stopping smoking. As none of the patients were current smokers, the study can provide no useful information on the impact of smoking status on erlotinib PK.

For the 150 mg/day dose, values for the main PK parameters measured in this study were very similar to those reported in the US phase I study. This suggests that at the recommended dose, exposure to erlotinib is similar between Japanese and Western patients.

Suspected drug-induced lung injury, manifesting as interstitial pneumonitis was observed clinically in one patient who received erlotinib 100 mg/day. Although this toxicity is serious, the reported incidence of ILD was very low in studies of erlotinib in the USA and Europe; in a
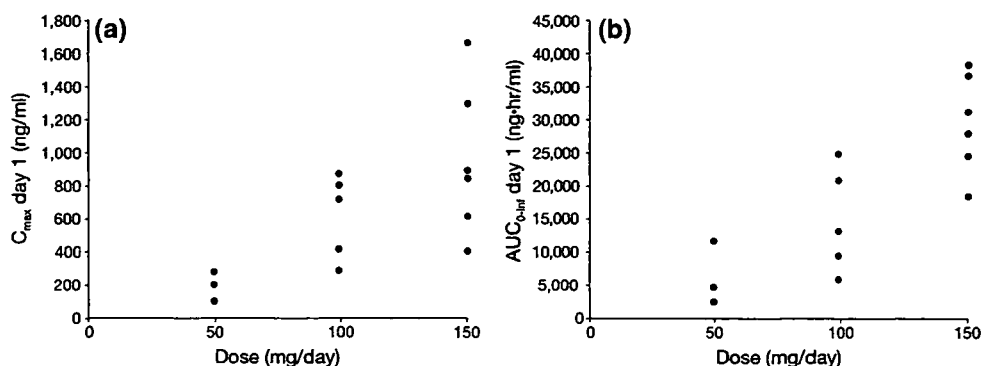
Fig. 3 $C_{max}$ (a) and $AUC_{0-inf}$ (b) according to erlotinib dose on day 1 following oral administration
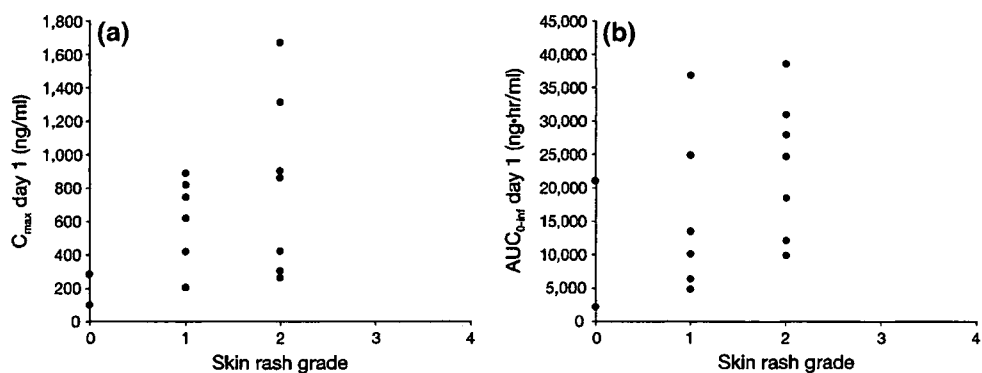


Fig. 4 Relationships between a rash and $C_{max}$ on day 1, and b rash and $AUC_{0-inf}$ on day 1

phase III study (BR.21) of erlotinib monotherapy in relapsed NSCLC, ILD occurred at the same incidence in the erlotinib and placebo arms (0.8%) [19]. ILD has also been reported with gefitinib, another EGFR tyrosine-kinase inhibitor [11, 22]. In patients treated with gefitinib, the onset of ILD is generally acute (i.e. within 4 weeks of treatment) and the incidence has been reported as 5.8% in Japanese patients [27]. The reported incidence of ILD with gefitinib is higher in Japan than elsewhere, although the reason for this is unknown. This may represent a greater prevalence of the toxicity, greater awareness and reporting, or an increased genetic susceptibility in the Japanese population. However, the biological mechanisms, such as environmental, clinical and genetic factors that may contribute to this toxicity have not yet been elucidated. Thus, further investigation to identify the mechanism of drug-induced interstitial pneumonitis associated with EGFR tyrosine-kinase inhibitors is warranted.

In the current trial, four of 11 evaluable patients (3 males and 1 female) achieved a partial response, all of whom had NSCLC of adenocarcinoma subtype. The three males were former smokers with more than 50 pack years. These results are particularly interesting as clinical characteristics that have been reported as favorable factors for clinical benefit with gefitinib and erlotinib in NSCLC patients include female gender, adenocarcinoma subtype, and never-smoking status [18, 22]. Our results are, however, not unexpected, as data from the placebo-controlled BR.21 study of erlotinib in relapsed NSCLC demonstrated that the survival benefit with erlotinib was not restricted to particular sub-populations [19]. Recently, it has been reported that certain mutations in the tyrosine-kinase domain of EGFR are present in a subset of NSCLCs, most commonly in patients who have never smoked, and these mutations appear to be associated with a greater likelihood of response to gefitinib and erlotinib [13, 16, 17]. Importantly, however, not all patients with mutations obtain a response, and some patients without mutations do obtain a response. The incidence of EGFR mutations in Japanese patients with NSCLC is about 40%, which is higher than that in Caucasian patients (10–15%) [13, 20]. However, any possible association between EGFR mutations and survival with EGFR tyrosine-kinase inhibitors is presently unclear. In a retrospective analysis of samples from the BR.21 study, the presence of EGFR mutations was significantly associated with response to erlotinib but not with survival [24, 25]. Other markers that are under investigation as potential predictors of clinical benefit with EGFR tyrosine-kinase inhibitors are EGFR expression and EGFR gene copy number [7]. None of these markers of EGFR status were assessed in

the current study, although such assessments would be important in future studies, including those restricted to Japanese patient populations.

In conclusion, the results of this study confirm that in Japanese patients, the recommended dose of erlotinib is 150 mg/day. At this dose level, erlotinib has acceptable toxicity with a PK profile similar to that seen in a US phase I study. Several partial responses were observed, all in patients with NSCLC, including male smokers. Analysis of the clinical benefits of erlotinib in Japanese patients with NSCLC entered into phase II/III trials are ongoing.

# References

 1. Akita RW, Sliwkowski MX (2003) Preclinical studies with erlotinib (Tarceva). Semin Oncol 30:15–24
 2. Bence AK, Anderson EB, Halepota MA, Doukas MA, DeSimone PA, Davis GA, Smith DA, Koch KM, Stead AG, Mangum S, Bowen CJ, Spector NL, Hsieh S, Adams VR (2005) Phase I pharmacokinetic studies evaluating single and multiple doses of oral GW572016, a dual EGFR-ErbB2 inhibitor, in healthy subjects. Invest New Drugs 23:39–49
 3. Bonomi P (2003) Clinical studies with non-iressa EGFR tyrosine kinase inhibitors. Lung Cancer 41(1):S43–S48
 4. Bulgaru AM, Mani S, Goel S, Perez-Solar R (2003) Erlotinib (Tarceva): a promising drug targeting epidermal growth factor receptor tyrosine kinase. Expert Rev Anticancer Ther 3:269–279
 5. Carpenter G, Cohen S (1990) Epidermal growth factor. J Biol Chem 265:7709–7712
 6. Faber MS, Fuhr U (2004) Time response of cytochrome P450 1A2 activity on cessation of heavy smoking. Clin Pharmacol Ther 76:178–184
 7. Giaccone G (2005) HER1/EGFR targeted agents: predicting the future for patients with unpredictable outcomes to therapy. Ann Oncol 16:538–548
 8. Hamilton M, Wolf JL, Rusk J, Beard SE, Clark GM, Witt K, Cagnoni PJ (2006) Effects of smoking on the pharmacokinetics of erlotinib. Clin Cancer Res 12:2166–2171
 9. Hidalgo M (2003) Erlotinib: preclinical investigations. Oncology (Huntingt) 17:11–16
10. Hidalgo M, Siu LL, Nemunaitis J, Rizzo J, Hammond LA, Takimoto C, Eckhardt SG, Tolcher A, Britten CD, Denis L, Ferrante K, Von Hoff DD, Silberman S, Rowinsky EK (2001) Phase I and pharmacologic study of OSI-774, an epidermal growth factor receptor tyrosine kinase inhibitor, in patients with advanced solid malignancies. J Clin Oncol 19:3267–3279
11. Inoue A, Saijo Y, Maemondo M, Gomi K, Tokue Y, Kimura Y, Ebina M, Kikuchi T, Moriya T, Nukiwa T (2003) Severe acute interstitial pneumonia and gefitinib. Lancet 361:137–139
12. Jorissen RN, Walker F, Pouliot N, Garrett TP, Ward CW, Burgess AW (2003) Epidermal growth factor receptor: mechanisms of activation and signalling. Exp Cell Res 284:31–53
13. Kosaka T, Yatabe Y, Endoh H, Kuwano H, Takahashi T, Mitsudomi T (2004) Mutations of the epidermal growth factor receptor gene in lung cancer: biological and clinical implications. Cancer Res 64:8919–8923
14. Lepper ER, Swain SM, Tan AR, Figg WD, Sparreboom A (2003) Liquid-chromatographic determination of erlotinib (OSI-774), an epidermal growth factor receptor tyrosine kinase inhibitor. J Chromatogr B Analyt Technol Biomed Life Sci 796:181–188
15. Nakagawa K, Tamura T, Negoro S, Kudoh S, Yamamoto N, Yamamoto N, Takeda K, Swaisland H, Nakatani I, Hirose M, Dong RP, Fukuoka M (2003) Phase I pharmacokinetic trial of the selective oral epidermal growth factor receptor tyrosine kinase inhibitor gefitinib ('Iressa', ZD1839) in Japanese patients with solid malignant tumors. Ann Oncol 14:922–930
16. Paez JG, Janne PA, Lee JC, Tracy S, Greulich H, Gabriel S, Herman P, Kaye FJ, Lindeman N, Boggon TJ, Naoki K, Sasaki H, Fujii Y, Eck MJ, Sellers WR, Johnson BE, Meyerson M (2004) EGFR mutations in lung cancer: correlation with clinical response to gefitinib therapy. Science 304:1497–1500
17. Pao W, Miller V, Zakowski M, Doherty J, Politi K, Sarkaria I, Singh B, Heelan R, Rusch V, Fulton L, Mardis E, Kupfer D, Wilson R, Kris M, Varmus H (2004) EGF receptor gene mutations are common in lung cancers from "never smokers" and are associated with sensitivity of tumors to gefitinib and erlotinib. Proc Natl Acad Sci USA 101:13306–13311
18. Perez-Soler R, Chachoua A, Hammond LA, Rowinsky EK, Huberman M, Karp D, Rigas J, Clark GM, Santabarbara P, Bonomi P (2004) Determinants of tumor response and survival with erlotinib in patients with non-small-cell lung cancer. J Clin Oncol 22:3238–3247
19. Shepherd FA, Rodrigues Pereira J, Ciuleanu T, Tan EH, Hirsh V, Thongprasert S, Campos D, Maoleekoonpiroj S, Smylie M, Martins R, van Kooten M, Dediu M, Findlay B, Tu D, Johnston D, Bezjak A, Clark G, Santabarbara P, Seymour L, National Cancer Institute of Canada Clinical Trials Group (2005) Erlotinib in previously treated non-small-cell lung cancer. N Engl J Med 353:123–132
20. Shigematsu H, Lin L, Takahashi T, Nomura M, Suzuki M, Wistuba II, Fong KM, Lee H, Toyooka S, Shimizu N, Fujisawa T, Feng Z, Roth JA, Herz J, Minna JD, Gazdar AF (2005) Clinical and biological features associated with epidermal growth factor receptor gene mutations in lung cancers. J Natl Cancer Inst 97:339–346
21. Sridhar SS, Seymour L, Shepherd FA (2003) Inhibitors of epidermal-growth-factor receptors: a review of clinical research with a focus on non-small-cell lung cancer. Lancet Oncol 4:397–406
22. Takano T, Ohe Y, Kusumoto M, Tateishi U, Yamamoto S, Nokihara H, Yamamoto N, Sekine I, Kunitoh H, Tamura T, Kodama T, Saijo N (2004) Risk factors for interstitial lung disease and predictive factors for tumor response in patients with advanced non-small cell lung cancer treated with gefitinib. Lung Cancer 45:93–104
23. Therasse P, Arbuck SG, Eisenhauer EA, Wanders J, Kaplan RS, Rubinstein L, Verweij J, Van Glabbeke M, van Oosterom AT, Christian MC, Gwyther SG (2000) New guidelines to evaluate the response to treatment in solid tumors. European Organization for Research and Treatment of Cancer, National Cancer Institute of the United States, National Cancer Institute of Canada. J Natl Cancer Inst 92:205–216
24. Tsao MS, Kamel-Reid S, Shepherd FA (2006) Assessing EGFR mutations. N Engl J Med 354:527–528
25. Tsao MS, Sakurada A, Cutz JC, Zhu CQ, Kamel-Reid S, Squire J, Lorimer I, Zhang T, Liu N, Daneshmand M, Marrano P, da Cunha Santos G, Lagarde A, Richardson F, Seymour L, Whitehead M, Ding K, Pater J, Shepherd FA (2005) Erlotinib in lung cancer—molecular and clinical predictors of outcome. N Engl J Med 353:133–144
26. Wikstrand CJ, Bigner DD (1998) Prognostic applications of the epidermal growth factor receptor and its ligand, transforming growth factor-alpha. J Natl Cancer Inst 90:799–801
27. Yoshida S (2005) The results of gefitinib prospective investigation. Med Drug J 41:772–789

# Prospective Study of Positron Emission Tomography for Evaluation of the Activity of Lapatinib, a Dual Inhibitor of the ErbB1 and ErbB2 Tyrosine Kinases, in Patients with Advanced Tumors

**Kenji Kawada[1], Koji Murakami[2], Takashi Sato[2], Yoshiki Kojima[2], Hiromichi Ebi[1], Hirofumi Mukai[1,], Makoto Tahara[1], Kaoru Shimokata[3] and Hironobu Minami[1]**

[1]Department of Oncology/Hematology, National Cancer Center Hospital East, Kashiwa, [2]Department of Diagnostic Radiology, National Cancer Center Hospital East, Kashiwa and [3]Department of Respiratory Medicine, Nagoya University Graduate School of Medicine, Nagoya, Japan

**Background:** To evaluate the role of FDG-PET in assessing anti-tumor efficacy of molecular targeted drugs, we prospectively performed FDG-PET and CT for response evaluation in patients treated with lapatinib, a dual inhibitor of ErbB1 and ErbB2 tyrosine kinases.
**Methods:** Lapatinib was given orally once a day at doses ranging from 1200 to 1800 mg in a phase I study. CT and FDG-PET were performed before treatment, and at 1, 2 and 3 months after the initiation of the treatment and every 2 months thereafter.
**Results:** A total of 29 FDG-PET examinations were performed in eight patients with various solid tumors and the metabolic activity in the tumor was evaluated as SUVmax. The best responses, as assessed by CT, were as follows; one partial response, four stable disease and three disease progression. The partial response was observed in a patient with trastuzumab-resistant breast cancer, whose SUVmax was decreased by 60% from baseline. In all of the four patients whose best response was stable disease, the SUVmax was decreased by 6–42% one month after the start of treatment. Prolonged stable disease (10 months) was observed in a patient with colon cancer, whose SUVmax was decreased by 42%. In the patient group with disease progression, SUVmax was increased in two out of three patients.
**Conclusions:** FDG-PET detected decreases in the metabolic activity of the tumors in patients who experienced clinical benefits on treatment with lapatinib. Thus, FDG-PET may be useful for the evaluation of molecular targeted drugs, such as lapatinib.

*Key words: FDG-PET — lapatinib — phase I — pharmacodynamics — biomarker*

## INTRODUCTION

Recently, many molecular targeted drugs that act as cytostatic, rather than cytotoxic, agents have been developed. It is expected that they may slow or stop the growth of tumors, without causing existing tumors to shrink. Furthermore, their toxicities are expected to be mild. Therefore, toxicity and decrease in tumor size may not be used as endpoints in phase I and phase II studies, respectively and new endpoints are necessary for the clinical trial of molecular targeted drugs.

Positron emission tomography with the glucose analog fluorine-18 fluorodeoxyglucose (FDG-PET) allows the noninvasive serial measurements of glucose metabolism in tumors. In oncology, FDG-PET was first used for the diagnosis and staging of tumors. FDG uptake is closely related to the number and proliferative capacity of viable tumor cells (1,2). Therefore, treatment-induced changes resulting in tumor cell death or growth arrest leads to a reduction in FDG uptake. It has been reported that FDG-PET may be useful for the evaluation of anti-cancer treatments using cytotoxic chemotherapy (3–7). These data suggest that FDG-PET may offer a surrogate marker for clinical benefit in traditional chemotherapy. If molecular targeted drugs also inhibit the proliferation of cancer cells, reduction of FDG uptake by tumors should also occur after treatment with molecular targeted drugs. Therefore, FDG-PET can be expected to be a surrogate marker for the action of cytostatic molecular targeted drugs as well.

For reprints and all correspondence: Hironobu Minami, Department of Oncology/Hematology, National Cancer Center Hospital East, 6-5-1 Kashiwanoha, Kashiwa, Chiba, 277-8577, Japan.
E-mail: hminami@east.ncc.go.jp

Lapatinib is a new drug that inhibits the epidermal growth factor receptor tyrosine kinases ErbB1 and ErbB2. By inhibiting signals from these receptors, lapatinib blocks several downstream pathways involved in cell proliferation, invasion and apoptosis, such as ERK-1/2 and AKT, respectively. Phase I trials have been conducted in the USA (8), but the maximum tolerated dose was not determined because lapatinib was generally well tolerated. Biological activities, including partial responses in patients with trastuzumab-resistant breast cancer and disease stabilization of a variety of carcinomas, were reported. A phase I clinical trial has been conducted in patients with solid tumors in Japan (9). To evaluate the efficacy of lapatinib by FDG-PET and to correlate the results of FDG-PET with response evaluation by CT, FDG-PET was prospectively performed in a subsidiary study. This communication is therefore a report of the FDG-PET study conducted in association with a phase I study of lapatinib, details of which will be reported separately.

## PATIENTS AND METHODS

### PATIENTS AND TREATMENT

This phase I study was conducted in two institutions, Kinki University Hospital and the National Cancer Center Hospital East. Lapatinib was administered orally once daily until patients had disease progression or unacceptable toxicities. Six patients per dose were treated at 900, 1200, 1600 or 1800 mg/day. At the National Cancer Center Hospital East, three patients per group received 1200, 1600 or 1800 mg/day. Of these nine patients, eight were enrolled in the FDG-PET study. The protocols of the phase I study and the FDG-PET study were approved by the Institutional Review Board of the National Cancer Center. Written informed consent was obtained from each patient.

### EVALUATION OF TUMOR RESPONSES

At study entry, up to three representative lesions were selected for tumor evaluation. The sum of the largest diameter of each of these lesions was assessed with CT and the maximum standardised uptake values (SUVmax), which is the maximum pixel value within the region of interest, of the same lesions were recorded with FDG-PET. CT and FDG-PET were performed before treatment, and at 1, 2 and 3 months after the initiation of the treatment and every 2 months thereafter. Responses by CT were classified according to the response evaluation criteria in solid tumors (RECIST). Treatment discontinuation owing to disease progression was based on CT findings according to the protocol of the phase I study. The results of the PET analysis were not taken into account for this purpose.

Time to progression was defined as the time from first dose of lapatinib to the earliest documentation of progression, death from any cause, or withdrawal from the trial for any reason.

FDG-PET was performed using a GE-Advanced scanner (General Electric Medical Systems, Milwaukee, WI, USA) with an axial field of view of 15 cm and a slice thickness of 4.75 mm. The SUVmax is known to be affected by several factors, including plasma glucose levels, time from FDG injection to measurement and body weight. Therefore, all patients fasted for at least 6 h before FDG-PET scanning and plasma glucose level was measured just before the FDG injection. Exactly 60 min after intravenous injection of 259–310 MBq FDG, an attenuation-corrected whole body scan was acquired in seven bed positions (5-min emission and 1-min transmission).

## RESULTS

A total of 29 FDG-PET examinations were performed in eight patients whose characteristics are listed in Table 1. All patients had prior chemotherapy and four patients with non-small cell lung cancer had failed gefitinib treatment.

Time from FDG injection to the start of PET scanning was exactly 60 min in 28 examinations and 59 min on one occasion. Plasma glucose levels were always below 120 mg/dl (median, 97 mg/dl; range, 77–116). Little change in body weight of individual patients was observed during the course of the study.

The median number of days between pretreatment FDG-PET and treatment initiation was 4 (range, 1–12) days. In 93% of examinations, CT and FDG-PET were performed within 7 days; the median number of days between CT and FDG-PET examination was 1 (range, 0–21 days).

The best responses, as assessed by CT, were as follows; one partial response, four stable disease and three disease progression. Figure 1 shows the time course of the SUVmax and tumor responses in each patient.

The single partial response was observed in a patient with trastuzumab-resistant breast cancer (Her2, 3+; ER/PgR, negative) receiving 1600 mg/day, whose SUVmax was decreased by 60% from baseline one month after the start of treatment when a partial response was documented by CT; thereafter, SUVmax began to increase again 2 months before progression was documented by CT (Fig. 2A, B).

In all four patients whose best response was stable disease, the SUVmax was decreased by 6–42% 1 month after the start of treatment. In a patient with colon cancer with prolonged stable disease (10 months), the SUVmax was decreased by 42% at the first post-treatment evaluation and maintained thereafter for 9 months. The SUVmax also began to increase 1 month earlier than the documentation of disease progression by CT (Fig. 3A, B).

In the patient group with disease progression, the best SUVmax response ranged from +5% to −42%. SUVmax was increased by 4–5% in two out of three patients with CT-assessed progressive disease (Fig. 1). In a patient whose

Table 1. Patient characteristics and response to lapatinib

| No. | Dose (mg) | Age (years) | Sex | Tumor type | P.S.* | No. of prior regimens of chemotherapy | Response to lapatinib | TTP† days |
|---|---|---|---|---|---|---|---|---|
| 1 | 1200 | 49 | F | NSCLC‡ | 1 | 4 | SD | 103 |
| 2 | 1200 | 61 | M | Sarcoma | 1 | 1 | PD | 20 |
| 3 | 1200 | 50 | M | CRC§ | 0 | 2 | PD | 48 |
| 4 | 1600 | 55 | F | Breast cancer | 0 | 3 | PR | 132 |
| 5 | 1600 | 61 | M | NSCLC‡ | 1 | 3 | SD | 98 |
| 6 | 1600 | 65 | M | CRC§ | 0 | 2 | SD | 335 |
| 7 | 1800 | 53 | M | NSCLC‡ | 1 | 4 | PD | 34 |
| 8 | 1800 | 37 | F | NSCLC‡ | 0 | 3 | SD | 110¶ |

F, female; M, male.
*Performance status.
†Time to progression.
‡Non-small-cell lung cancer.
§Colorectal cancer.
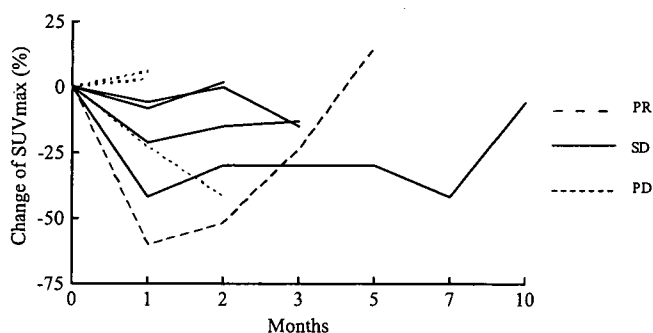¶Withdrawn from study without progression.



Figure 1. The time course of the SUVmax and tumor responses in eight patients.

SUVmax was decreased in spite of disease progression documented by CT, the selected targeted lesions were stable disease assessed by CT, but a new lesion appeared 2 months after the start of treatment.

## DISCUSSION

Molecular targeted drugs aim at tumor growth stabilization rather than tumor shrinkage and no major volume changes are expected. In addition, the mechanism of action of some of these agents may be such that higher doses beyond a certain level may offer no additional benefit. With traditional cytotoxic drugs, increasing doses lead to increasing efficacy; thus, the recommended dose of cytotoxic agents has been routinely determined on the basis of toxicities in phase I studies. However, for molecular targeted drugs, the appropriate approach to determine recommended doses for further clinical trials has not yet been established, because toxicities of these drugs are not necessarily considered to correlate with their anti-tumor activity (10). Similarly, conventional
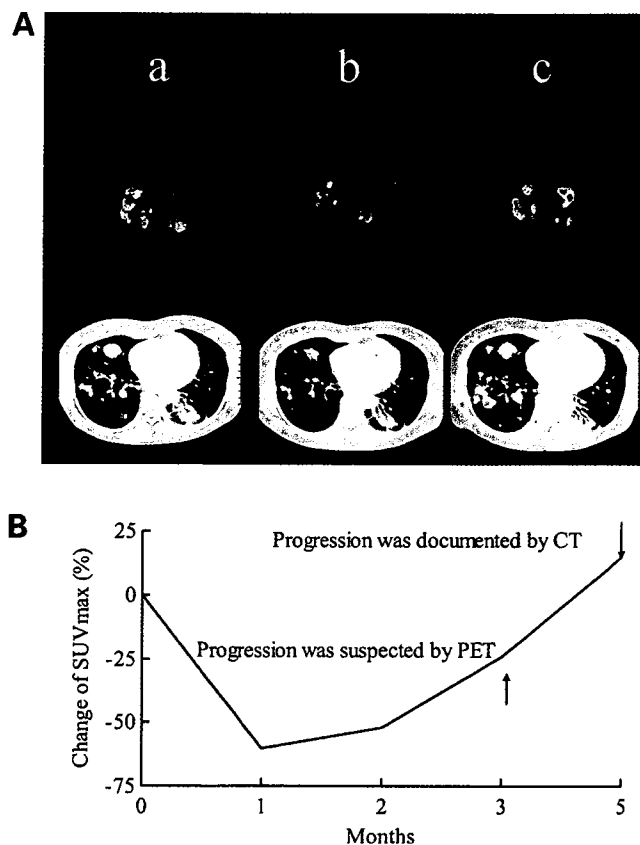


Figure 2. (A) Comparison of FDG-PET and CT with trastuzumab-resistant breast cancer with lung metastases. Partial response was documented by CT. a, before the treatment; b, the major reduction in FDG uptake and objective tumor response was observed after 1 month of treatment; c, disease progression was confirmed by CT after 5 months of treatment. (B) The time course of the SUVmax and tumor response in a patient with breast cancer with partial response was documented by CT. The SUVmax was decreased by 60% from baseline after 1 month of treatment. The SUVmax began to increase 2 months before progression was documented by CT.
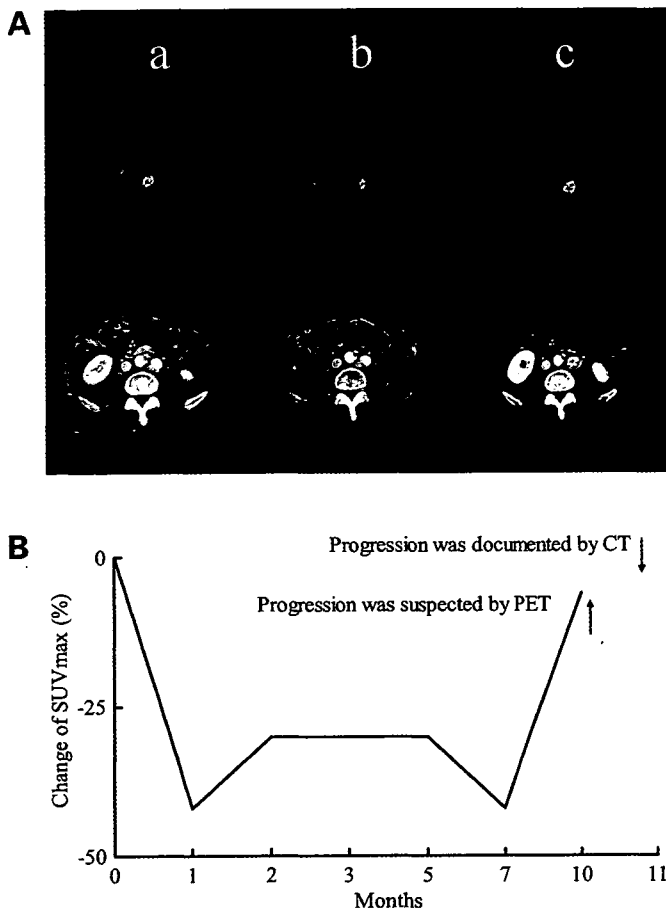
**A**



**B**



Figure 3. (A) Comparison of FDG-PET and CT with colorectal cancer with para-aortic lymph node metastases. Prolonged stable disease was documented by CT. a, before the treatment; b, the major reduction in FDG uptake was observed after 1 month of treatment, but no volume change was observed by CT; c, progression in FDG uptake was observed after 10 months of treatment, but no major volume change was observed by CT. (B) The time course of the SUVmax and tumor response in a patient with colorectal cancer with prolonged stable disease. The SUVmax was decreased by 42% from baseline after 1 month treatment, and maintained thereafter for 9 months. The SUVmax also began to increase 1 month earlier than the documentation of disease progression by CT.

strategies to evaluate anti-tumor activity in phase II studies may not be useful for molecular targeted drugs, because these agents may not cause a reduction in tumor size. The following approaches have been used to determine the appropriate dose of molecular targeted drugs for further clinical trials: (i) pharmacokinetic data in patients have been compared with the results of preclinical studies; (ii) changes in the targeted molecules in tumors or surrogate tissues have been evaluated; and (iii) the maintenance of stable disease has been suggested to be a marker of activity in the development of these new agents (11). However, thus far none of these parameters has been established as an endpoint for phase I studies.

In successful clinical trials of molecular targeted drugs such as trastuzumab (12), rituximab (13), imatinib (14), gefitinib (15), erlotinib (16) and sorafenib (17), tumor shrinkage

was in fact observed. However, the relatively low response rates to these compounds may not fully explain the increased progression-free or overall survival observed in phase III studies. Furthermore, as discussed above, other molecular targeted drugs may not cause tumor shrinkage but induce tumor growth inhibition with mild toxicities. It is difficult to evaluate anti-tumor activity of these agents in phase II studies by the methodology established for cytotoxic drugs. The clinical value of any new agent must be documented in randomized phase III studies. If phase III trials were to be conducted without any preliminary evidence of efficacy, available patients and financial resources would be insufficient to test all new cytostatic agents under clinical evaluation. Therefore, other surrogate markers for response assessment are required in the clinical development of molecular targeted drugs to permit more efficient evaluation of cancer treatment. With such an approach, the most promising agents could be moved forward quickly, with less effective agents rapidly identified and discarded. FDG-PET is expected to be a surrogate marker for the action of cytostatic molecular targeted drugs.

A correlation between treatment efficacy and glucose metabolism in patients has been reported for imatinib therapy. FDG-PET could be used as an early and sensitive method to evaluate the response of gastrointestinal stromal tumors to imatinib mesylate treatment (18). FDG-PET data obtained 8 days after imatinib treatment correlated with symptom control as well as progression-free survival. It was also reported that micro-PET imaging with FDG could be used for monitoring the effect of PKI-166, another dual inhibitor of ErbB1 and ErbB2, in preclinical studies (19). The mechanism of action of PKI-166 is similar to lapatinib, which is also a dual inhibitor of ErbB1 and ErbB2.

The results of our study concurred with the findings of previous studies. The effect of lapatinib was evaluated by FDG-PET in eight patients, and clinical benefits of treatment, such as partial response and prolonged stable disease, were observed in the two patients with the greatest decrease in the SUVmax. The SUVmax was minimally or moderately decreased by treatment in all four patients whose best response was stable disease. The SUVmax was increased in two out of three patients with disease progression detected by CT. In the other patient with disease progression documented by CT, the SUVmax was decreased. In this case a new lesion appeared while the selected targeted lesions were stable. This may be due to the heterogeneity within different lesions of the same cancer.

At the present time, there are no standard criteria for evaluation by FDG-PET, although recommendations were published in 1999 by the European Organization for Research and Treatment of Cancer (EORTC) (7). In the EORTC recommendations, progressive metabolic disease is classified as an increase in standard uptake value greater than 25%, and partial metabolic response as a decrease in standard uptake value greater than 25% after more than one treatment cycle. SUVmax is influenced by factors such as

the time from FDG injection to measurement, plasma glucose level, body weight and partial volume effect (20). It was reported that the variability of FDG uptake as assessed by SUVmax without treatment is less than 20% (21). Therefore, it was proposed that a significant change in SUVmax for the evaluation of anti-tumor activity of chemotherapeutic agents should be above the 25% threshold (22). In the present study, SUVmax decreased by more than 25% in four patients, two of whom experienced significant clinical benefit, while the other two had stable disease and disease progression.

The usefulness of FDG-PET in evaluating the anti-tumor activity of lapatinib is suggested by the results of the present investigation. However, this was a small exploratory study, and its confirmation awaits the results of larger studies. Further studies should be conducted in conjunction with phase II or phase III trials in which patients with the same tumor types are treated in a uniform way. Moreover, it will be necessary to show that the response evaluated by FDG-PET is predictive of a clinical endpoint, such as survival.

In conclusion, FDG-PET may be useful for the evaluation of molecular targeted drugs, such as lapatinib. However, this will need further validation in phase II or phase III studies in patients with the same types of tumors.

## Conflict of interest statement

None declared.

## References

1. Higashi K, Clavo AC, Wahl RL. Does FDG uptake measure proliferative activity of human cancer cells? *In vitro* comparison with DNA flow cytometry and tritiated thymidine uptake. *J Nucl Med* 1993;34:414–9.
2. Minn H, Joensuu H, Ahonen A, Klemi P. Fluorodeoxyglucose imaging: a method to assess the proliferative activity of human cancer *in vivo*. Comparison with DNA flow cytometry in head and neck tumors. *Cancer* 1988;61:1776–81.
3. Cohade C, Wahl RL. PET scanning and measuring the impact of treatment. *Cancer J* 2002;8:119–34.
4. MacManus MP, Hicks RJ, Matthews JP, McKenzie A, Rischin D, Salminen EK, et al. Positron emission tomography is superior to computed tomography scanning for response-assessment after radical radiotherapy or chemoradiotherapy in patients with non-small-cell lung cancer. *J Clin Oncol* 2003;21:1285–92.
5. Stokkel MP, Draisma A, Pauwels EK. Positron emission tomography with 2-[18F]-fluoro-2-deoxy-D-glucose in oncology. Part IIIb: Therapy response monitoring in colorectal and lung tumours, head and neck cancer, hepatocellular carcinoma and sarcoma. *J Cancer Res Clin Oncol* 2001;127:278–85.
6. van der Hiel B, Pauwels EK, Stokkel MP. Positron emission tomography with 2-[18F]-fluoro-2-deoxy-D-glucose in oncology. Part IIIa: Therapy response monitoring in breast cancer, lymphoma and gliomas. *J Cancer Res Clin Oncol* 2001;127:269–77.
7. Young H, Baum R, Cremerius U, Herholz K, Hoekstra O, Lammertsma, et al. European Organization for Research and Treatment of Cancer (EORTC) PET Study Group. Measurement of clinical and subclinical tumour response using [$^{18}$F]-fluorodeoxyglucose and positron emission tomography: review and 1999 EORTC recommendations. *Eur J Cancer* 1999;35:1773–82.
8. Burris HA, 3rd, Hurwitz HI, Dees EC, Dowlati A, Blackwell KL, O'Neil B, et al. Phase I safety, pharmacokinetics, and clinical activity study of lapatinib (GW572016), a reversible, dual inhibitor of epidermal growth factor receptor tyrosine kinases in heavily pretreated patients with metastatic carcinomas. *J Clin Oncol* 2005;23:5305–13.
9. Minami H, Nakagawa K, Kawada K, Mukai H, Tahara M, Kurata T, et al. A phase I study of GW572016 in patients with solid tumors. *Proc ASCO* 2004;23:3048.
10. Korn EL, Arbuck SG, Pluda JM, Simon R, Kaplan RS, Christian MC. Clinical trial designs for cytostatic agents: are new approaches needed? *J Clin Oncol* 2001;19:265–72.
11. Schilsky RL. End points in cancer clinical trials and the drug approval process. *Clin Cancer Res* 2002;8:935–38.
12. Baselga J, Tripathy D, Mendelsohn J, Baughman S, Benz CC, Dantis L, et al. Phase II study of weekly intravenous trastuzumab (Herceptin) in patients with HER2/neu-overexpressing metastatic breast cancer. *Semin Oncol* 1999;26:78–83.
13. Maloney DG, Grillo-Lopez AJ, Bodkin DJ, White CA, Liles TM, Royston I, et al. IDEC-C2B8: results of a phase I multiple-dose trial in patients with relapsed non-Hodgkin's lymphoma. *J Clin Oncol* 1997;15:3266–74.
14. Druker BJ, Talpaz M, Resta DJ, Peng B, Buchdunger E, Ford JM, et al. Efficacy and safety of a specific inhibitor of the BCR-ABL tyrosine kinase in chronic myeloid leukemia. *N Engl J Med* 2001;344:1031–7.
15. Fukuoka M, Yano S, Giaccone G, Tamura T, Nakagawa K, Douillard JY, et al. Multi-institutional randomized phase II trial of gefitinib for previously treated patients with advanced non-small-cell lung cancer. *J Clin Oncol* 2003;21:2237–46.
16. Perez-Soler R, Chachoua A, Hammond LA, Rowinsky EK, Huberman M, Karp D, et al. Determinants of tumor response and survival with erlotinib in patients with non-small-cell lung cancer. *J Clin Oncol* 2005;22:3238–47.
17. Escudier B, Szczylik C, Eisen T, Stadler WM, Schwartz B, Shan M, et al. Randomized phase III trial of the Raf kinase and VEGFR inhibitor sorafenib (BAY43-9006) in patients with advanced renal cell carcinoma. *Proc ASCO* 2005;41:4510.
18. Stroobants S, Goeminne J, Seegers M, Dimitrijevic S, Dupont P, Nuyts J, et al. $^{18}$FDG-Positron emission tomography for the early prediction of response in advanced soft tissue sarcoma treated with imatinib mesylate (Glivec). *Eur J Cancer* 2003;39:2012–20.
19. Christian W, Arash S, Ingo M. Effects of PKI-166 on A-431 vulvar carcinoma in SCID mice assessed with microPET using 18F-FLT and 18F-FDG. *Proc AACR* 2003;94:6190.
20. Keyes JW, Jr. SUV: standard uptake or silly useless value? *J Nucl Med* 1995;36:1836–9.
21. Weber WA, Ziegler SI, Thodtmann R, Hanauske AR, Schwaiger M. Reproducibility of metabolic measurements in malignant tumors using FDG PET. *J Nucl Med* 1999;40:1771–7.
22. Minn H, Zasadny KR, Quint LE, Wahl RL. Lung cancer: reproducibility of rquantitative measurements for evaluating 2-[F-18]-fluoro-2-deoxy-D-glucose uptake at PET. *Radiology* 1995;196:167–73.

# CYP2C8 haplotype structures and their influence on pharmacokinetics of paclitaxel in a Japanese population

Yoshiro Saito[a], Noriko Katori[a], Akiko Soyama[a], Yukiko Nakajima[a], Takashi Yoshitani[a], Su-Ryang Kim[a], Hiromi Fukushima-Uesaka[a], Kouichi Kurose[a], Nahoko Kaniwa[a], Shogo Ozawa[a], Naoyuki Kamatani[b], Kazuo Komamura[g,h], Shiro Kamakura[h], Masafumi Kitakaze[h], Hitonobu Tomoike[h], Kenji Sugai[c], Narihiro Minami[c,d], Hideo Kimura[d], Yu-ichi Goto[d], Hironobu Minami[i], Teruhiko Yoshida[e], Hideo Kunitoh[f], Yuichiro Ohe[f], Noboru Yamamoto[f], Tomohide Tamura[f], Nagahiro Saijo[i] and Jun-ichi Sawada[a]

**Objective** CYP2C8 is known to metabolize various drugs including an anticancer drug paclitaxel. Although large interindividual differences in CYP2C8 enzymatic activity and several nonsynonymous variations were reported, neither haplotype structures nor their associations with pharmacokinetic parameters of paclitaxel were reported.

**Methods** Haplotype structures of the *CYP2C8* gene were inferred by an expectation-maximization based program using 40 genetic variations detected in 437 Japanese patients, which included cancer patients. Associations of the haplotypes and paclitaxel pharmacokinetic parameters were analyzed for 199 paclitaxel-administered cancer patients.

**Results** Relatively strong linkage disequilibriums were observed throughout the *CYP2C8* gene. We estimated 40 haplotypes without an amino-acid change and nine haplotypes with amino acid changes. The 40 haplotypes were classified into six groups based on network analysis. The patients with heterozygous *IG* group haplotypes harboring several intronic variations showed a 2.5-fold higher median area under concentration–time curve of C3′-p-hydroxy-paclitaxel and a 1.6-fold higher median value of C3′-p-hydroxy-paclitaxel/paclitaxel area under concentration–time curve ratio than patients bearing no *IG* group haplotypes (P<0.001 for both comparisons by Mann–Whitney U-test). No statistically significant differences, however, were observed between patients with and without the *IG* group (haplotypes) in clearance and area under

concentration–time curve of paclitaxel, area under concentration–time curve of 6α-hydroxy-paclitaxel and 6α-, C3′-p-dihydroxy-paclitaxel, and area under concentration–time curve ratio of 6α-hydroxy-paclitaxel/paclitaxel.

**Conclusion** CYP2C8*IG group haplotypes were associated with increased area under concentration–time curve of C3′-p-hydroxy-paclitaxel and area under concentration–time curve ratio of C3′-p-hydroxy-paclitaxel/paclitaxel. Thus, *IG group haplotypes might be associated with reduced CYP2C8 activity, possibly through its reduced protein levels. *Pharmacogenetics and Genomics* 17:461–471 © 2007 Lippincott Williams & Wilkins.

## Introduction

Cytochrome P450s (CYPs) catalyze oxidative metabolism of a wide variety of exogenous chemicals and endogenous compounds. Human CYP2C subfamily consists of four members, CYP2C18, CYP2C19, CYP2C9, and CYP2C8, all of which are located in tandem on chromosome 10q23–24 in the order listed above [1]. CYP2C8 is a clinically important enzyme, which metabolizes various drugs such as the anticancer drug paclitaxel (PTX), the antiarrhythmic drug amiodarone, the insulin secretagogue repaglinide, the HMG-CoA reductase inhibitor cerivastatin, and the nonsteroidal antiinflammatory drug ibuprofen [1]. This enzyme is also involved in the oxidation of retinoids and fatty acids including arachidonic acid [1].

Up to 38-fold interindividual variability has been reported on PTX 6α-hydroxylation and rosiglitazone *p*-hydroxylation and *N*-desmethylation by CYP2C8 [2,3]. Effects of CYP2C8 genetic polymorphisms on metabolic activities have also been studied. Two polymorphisms first identified were 805A > T (Ile269Phe, *CYP2C8*2*) and 416G > A/1196A > G (Arg139Lys, Lys399Arg, *CYP2C8*3*). The *2 and *3 alleles were mainly found in Africans with 0.04–0.18 frequencies, and in Caucasians with 0.10–0.23 frequencies, respectively [1]. Both alleles were associated with decreased enzymatic activities for PTX 6α-hydroxylation *in vitro* [4–6]. *CYP2C8*4* allele (792C > G, Ile264Met) was found in British Caucasians [6]. We found 475delA (*CYP2C8*5*) in Japanese, and this allele leads to a frame shift at codon 159 followed by a stop codon at residue 177 [7]. We also found five additional polymorphisms (*CYP2C8*6* to *10*) in Japanese [8]. Among them, *CYP2C8*7* (556C > T, Arg186X) and *8* (556C > G, Arg186Gly) are different nucleotide variations at the same position. The former variation results in the stop codon, and the latter leads to an amino-acid substitution with a markedly reduced hydroxylation activity to PTX *in vitro*. Recently, two additional variations, *CYP2C8*13* (669T > G, Ile223Met) and *14* (712G > C, Ala238Pro), have been reported [9].

To date, a few reports have shown the impact of *CYP2C8*3* alleles on drug pharmacokinetics. The presence of *3 was associated with reduced clearance and increased area under concentration-time curve (AUC) of (*R*)-ibuprofen [10]. In contrast, significantly reduced AUC and $C_{max}$ of repaglinide were observed in the patients with heterozygous *3 but not in patients with heterozygous *4 [11]. As for PTX, previous studies failed to show the influence of *CYP2C8* variations on PTX pharmacokinetics [12,13].

Haplotypes, linked polymorphisms on the same chromosome, often show more precise and strong association with phenotypes such as adverse reaction and/or pharmacokinetics of drugs than individual polymorphisms [14]. In this study, we determined/inferred haplotype structures of the *CYP2C8* gene using genetic polymorphisms detected in 437 Japanese patients. Then, association analysis was performed between the haplotypes and pharmacokinetic parameters for PTX and its metabolites. PTX is metabolized to form C3′-*p*-hydroxy-PTX (3′-*p*-OH-PTX) and 6α-hydroxy-PTX (6α-OH-PTX): both metabolites are further hydroxylated to 6α-,C3′-*p*-dihydroxy-PTX (diOH-PTX) [2,15,16]. CYP2C8 metabolizes PTX and 3′-*p*-OH-PTX into 6α-OH-PTX and diOH-PTX, respectively. Another enzyme, CYP3A4, metabolizes PTX and 6α-OH-PTX into 3′-*p*-OH-PTX and diOH-PTX, respectively. Previously, we showed that a *CYP3A4* haplotype affected the pharmacokinetics of these metabolites [9]. In this study, effects of *CYP2C8* haplotypes on PTX metabolism were investigated.

## Materials and methods
### Patients for DNA sequencing
A total of 437 Japanese patients (235 cancer patients administered PTX, 106 arrhythmic patients, and 96 epileptic patients) participated in this study. This population included 54 patients, who were previously used to identify the *CYP2C8*5* allele and four intronic variations [7], and seven patients with *CYP2C8*6* to *10* [8], *13* and *14* alleles [9]. Written informed consent was obtained from all participating patients. The ethical review boards of the National Cancer Center, the National Cardiovascular Center, the National Center of Neurology and Psychiatry, and the National Institute of Health Sciences approved this study.

### Polymerase chain reaction conditions and DNA sequencing
Genomic DNA was extracted from whole blood leukocytes. First, the entire *CYP2C8* gene except for −8.8 and −1.9 kb enhancer regions was amplified in two portions (from the promoter region to exon 5, and exons 6–9) using the primer sets listed in the 'first polymerase chain reaction (PCR)' section of Table 1. Amplification was performed from 200 ng of genomic DNA using 1.25 units of Z-T (Takara Bio. Inc., Shiga, Japan) with 0.2 μmol/l of the primer sets. The first PCR conditions were 30 cycles of 98°C for 5 s, 55°C for 5 s, and 72°C for 190 s. Then, each exon (except for simultaneous amplification of exons 2 and 3) was amplified by Ex-Taq (1.25 units) with a set of primers (0.2 μmol/l) listed in the 'second PCR' section of Table 1 (primers were designed in the intronic regions or promoter region). The second-round PCR conditions were 94°C for 5 min, followed by 30 cycles of 94°C for 30 s, 60°C for 1 min, and 72°C for 2 min, and then a final extension at 72°C for 7 min. As for the −8.8 and −1.9 kb enhancer regions, amplification was performed directly from 50 ng of genomic DNA under the same conditions as in the second round PCR. Thereafter, the PCR products were treated with a PCR Product Pre-Sequencing Kit (USB Co., Cleveland, Ohio, USA) and directly sequenced on both strands using an ABI BigDye Terminator Cycle Sequencing Kit (Applied Biosystems, Foster City, California, USA) with the primers listed in the 'Sequencing' section of Table 1. For the −8.8 and −1.9 kb enhancer regions, promoter region, exon 4, and exons 7–9, the primer sets for the second PCR were also utilized for sequencing. The excess dye was removed by a DyeEx 96 kit (Qiagen, Hilden, Germany). The eluates were applied to an ABI Prism 3700 DNA Analyzer (Applied Biosystems). All detected variations were confirmed by repeating the PCR from the genomic DNA and sequencing of the newly generated PCR products. Genbank accession number NT_030059.12 was used for the reference sequence. Under conditions used, the −8.8 kb enhancer region (pregnanex receptor/constitutive androstane receptor-binding site and its surrounding region), −1.9 kb enhancer region (glucocorticoid receptor-binding site and

**Table 1** Primers used for the sequencing of *CYP2C8*

| | Amplified and sequenced region | Forward primer | | Reverse primer | | Amplified length (bp) |
|---|---|---|---|---|---|---|
| | | Sequences (5'–3') | Position at 5'-end[b] | Sequences (5'–3') | Position at 5'-end[b] | |
| First PCR | Promoter to exon 5 | CTGTGGTGTAAGTGGTAATGAAC | 15578696 | AAAAGCCCTGAGAACCTATAATC | 15563106 | 15591 |
| | Exons 6–9 | TAAGTATTTGTCCCAGTGCTCTC | 15562092 | TAGCAACTATACAAGCACGGG | 15544271 | 17822 |
| Second PCR | – 8.8 kb | CCCAAAAAAGAGCAGGTGTAGCCAT | 15586590 | TTACTGTCTGTCAAGTGGACCTATC | 15586279 | 312 |
| | – 1.9 kb | CTGACCCACATTTTACTCAACTG | 15579731 | CCCAGTTTAGAGAGGAGAAAGTTAG | 15579471 | 261 |
| | Promoter | GTCCTGTTCTCCCAGAGTTTC | 15578600 | TCTCCAGAGTGAAAAGAGAAGC | 15577623 | 978 |
| | Exon 1 | TCATAAATTCCCAACTGGTC | 15578062 | GAGCTTGCAGTGAGTGGAGA | 15577279 | 784 |
| | Exons 2–3 | TGCTGAATGTGTTGAAGTGAGG | 15576234 | CTCCCTTGTCTCTGTGCTTC | 15575334 | 901 |
| | Exon 4 | AGGCAGTGGATGTGAATAACC | 15573481 | TCTGTACCTAAAGATTGGAGGCTG | 15572897 | 585 |
| | Exon 5 | TCTCAGCATACTATCACAAGGAC | 15567211 | TAAGGGCTATGTCAATGTGC | 15566208 | 1004 |
| | Exon 6 | ACTAACCTAAGCAGCGAATGA | 15554467 | TTTTCATCTCCCCACCACAGCATT | 15553696 | 772 |
| | Exon 7 | GGCTGGTTGTACTTCTGGAC | 15551500 | AATAGCAGAAAGTCCATCAAGC | 15551034 | 467 |
| | Exon 8 | GAAGTGATGAAATAGAGCGGCAA | 15547620 | TAGTGGCAGAGTTCAGTCAAACC | 15546922 | 699 |
| | Exon 9 | TGGGAATAAATAAAGAAATGACTG | 15545899 | GTCAGCATTAGAAAAGTATTAGCA | 15545166 | 734 |
| Sequencing[a] | Exon 1 | CAGTGTTTCTCCATCATCACAGC | 15577988 | TTCAGAGGGAGTATTTTGCTTT | 15577388 | |
| | Exon 2 | CATCACAGGCCATCTATAAGTGG | 15576165 | CCCCCTCACCCCAGTTACC | 15575764 | |
| | Exon 3 | GGTAACTGGGGTGAGGGGG | 15575782 | CTCCCTTGTCTCTGTGCTTC | 15575334 | |
| | Exon 5 | GGAACATTACACACTGGGGT | 15567115 | ATTATTTTTATTTCAAGAAGAGGG | 15566396 | |
| | Exon 6 | ACTAACCTAAGCAGCGAATGA | 15554467 | TCTCTGTCATCCTCCTCCATT | 15553904 | |

[a]Primer sets for the second PCR were used for the − 8.8 kb, − 1.9 kb, promoter, exons 4, 7, 8 and 9.
[b]The position in the reference sequence, NT_030059.12.

its surrounding region), promoter region (up to 890 bases upstream of the translational initiation site, including hepatocyte nuclear factor 4α-binding site) [17] and all nine exons and its flanking introns were successfully sequenced for all patients analyzed.

**Linkage disequilibrium and haplotype analyses**

Hardy–Weinberg equilibrium and linkage disequilibrium (LD) analyses were performed by SNPAlyze software (version 3.1, Dynacom Co., Yokohama, Japan), and a pairwise LD between variations was obtained for the $|D'|$ and rho square ($r^2$) values. Some haplotypes were unambiguously determined from patients with homozygous variations at all sites or a heterozygous variation at only one site. Separately, diplotypes (a combination of haplotypes) were inferred by LDSUPPORT software, which determines the posterior probability distribution of the diplotype configuration for each patient based on estimated haplotype frequencies [18]. Diplotypes of all patients were inferred with probabilities (certainties) of more than 0.95 except for 18 patients. Haplotypes without amino-acid changes were designated as *1, and haplotypes with amino-acid changes were numbered according to the assignments by the Human Cytochrome P450 (CYP) Allele Nomenclature Committee (*http://www.cypalleles.ki.se/cyp2c8.htm*). The estimated haplotypes (subtypes) were tentatively shown with numbers plus small alphabetical letters. The haplotypes (subtypes) already assigned by the Committee were described as numbers plus capital alphabetical letters (*1A*, *1B*, and *1C*). Network analysis was performed using haplotypes detected in more than two patients with Network 4.1.1.2 by median-joining algorithm (*http://fluxus-engineering.com/*) [19].

**Patients administered PTX and pharmacokinetic analysis**

Demographic data of 235 PTX-administered cancer patients including their eligibility criteria were described previously [9]. Of the 235 patients, 199 (185 nonsmall cell lung cancer, four thymic carcinoma, four breast cancer, and six other cancers) were treated with PTX at doses of 175–210 mg/m$^2$ (the high-dose group in the previous paper [9]) at the National Cancer Center, and used for analysis of associations between haplotypes and pharmacokinetic parameters. These patients consisted of 139 men and 60 women with a mean age of 60.8 (range: 29–81) years. All patients were naive to PTX and pretreated with dexamethasone and an antiallergic agent (diphenhydramine or chlorpheniramine maleate) as prophylactics against hypersensitivity reactions. Carboplatin or nedaplatin was coadministered to almost all patients immediately after PTX treatment. The ethical review boards of both the National Cancer Center and the National Institute of Health Sciences approved this study. Written informed consent was obtained from all patients.

Methods for pharmacokinetic analysis were described previously, and the parameters obtained previously were used for the current association studies [9].

**Statistical analysis for association studies**

Differences in medians of pharmacokinetic parameters were analyzed by the Kruskal–Wallis test or the Mann–Whitney $U$-test. Statistical analysis was done using Prism v.4.00 (GraphPad Software Inc., San Diego, California, USA) and SAS v.8.2 (SAS Institute Inc., Cary,

North Carolina, USA). A significance level of 0.05 was applied to all two-tailed analyses.

## Results

### CYP2C8 variations

We reported previously the *CYP2C8* nonsynonymous variations, *5 (475delA, 159fsX18) [7], *6 (511G > A, Gly171Ser), *7 (556C > T, Arg186X), *8 (556C > G, Arg186Gly,) *9 (740A > G, Lys247Arg), *10 (1149G > T, Lys383Asn) [8], *13 (669T > G, Ile223Met), and *14 (712G > C, Ala238Pro) [9]. These variations were, however, very rare in the Japanese, and it was rather difficult to perform statistical evaluation on their in-vivo associations with altered function, because of low frequencies [9]. Therefore, we continued resequencing this gene including the promoter and intronic regions for up to 437 patients. The enhancer regions were also sequenced for 199 patients administered PTX. Table 2 summarizes the obtained data, where Genbank accession number NT_030059.12 was utilized for the reference sequence. Forty variations, including 11 novel ones, were detected in 437 patients. Because we did not find any significant differences in the genotype distributions among the three disease types ($P \geq 0.05$ by $\chi^2$ test or Fisher's exact test), data from all patients were analyzed as one group. All detected variations were found in Hardy–Weinberg equilibrium ($P \geq 0.05$ by $\chi^2$ test or Fisher's exact test), except for two polymorphisms IVS3–97delT and IVS3–21_–20insT. These deviations were due to the occurrence of one extra homozygote, and the existence of these homozygotes was confirmed by amplification of DNA by another set of primers and resequencing (data not shown). The overall frequencies of the previously reported nonsynonymous variations *CYP2C8*5*, *6, *7, *8, *9, *10, *12 (1382_1384del TTG, del 461Val), *13, and *14 were 0.002, 0.002, 0.001, 0.001, 0.001, 0.001, 0.001, 0.001, and 0.001, respectively, and they were all found as heterozygotes. We also detected –271C > A (*CYP2C8*1B*) and –370T > G (*1C*) at frequencies of 0.106 and 0.330, respectively. The frequency of the *1C* allele in Japanese is approximately 5.4-fold higher than in Caucasians [6]. We did not detect any variation in the functional hepatocyte nuclear factor 4α-binding site (–155 to –137 from the translational start site on NT_030059.12) [17], and its surrounding region in 437 patients. Also no variation was found in pregnanex receptor/constitutive androstane receptor-binding site (–8807 to –8788), glucocorticoid receptor-binding site (–1930 to –1910) [17], and their surrounding regions in 199 PTX-administered patients.

### Linkage disequilibrium analysis

Using the 15 detected polymorphisms greater than 0.03 in frequency, LD was analyzed for $|D'|$ and $r^2$ values (Fig. 1). $|D'|$ values were more than 0.9 in 89 out of 105 (85%) combinations (Fig. 1, lower left). For $r^2$ values (Fig. 1, upper right), strong LD ($r^2 \geq 0.80$) was observed among IVS2-64A > G, IVS2–13_–12insT, IVS3 –166A > G, IVS4–150G > A, IVS4–94T > C, IVS6 + 196-

G > A, IVS7 + 49T > A, IVS8 + 106G > A, and 1497 (*24)C > T. These polymorphisms were also moderately linked with –411T > C and –370T > G ($r^2 \geq 0.49$). Strong LD was also observed between IVS3-21T > A and IVS4 + 151G > A ($r^2 = 0.93$), and both variations were partially linked with IVS8-204A > G ($r^2 \geq 0.57$). The $r^2$ values of the other combinations were below 0.33. Collectively, relatively strong LDs were observed throughout the *CYP2C8* gene, suggesting that one LD block covers the entire region analyzed (approximately 33 kb). Thus, *CYP2C8* haplotypes were analyzed as one block.

### Haplotype analysis

Haplotypes determined/inferred are shown in Fig. 2. The haplotypes obtained in this study were tentatively shown as a number plus small alphabetical letter except for the haplotypes already publicized on the Human Cytochrome P450 (*CYP*) Allele Nomenclature Committee website, which are described as the number plus capital alphabetical letter (*1A, *1B, and *1C). Several haplotypes were first unambiguously assigned by homozygous single nucleotide polymorphisms at all sites (*1d-*1f, *1j, and *1w) or a heterozygous single nucleotide polymorphism at only one site (*1k, *1m, *1t, *1z, *1aa, and *8b). Separately, diplotypes for each patient were inferred by LDSUPPORT software. The additionally inferred haplotypes were 27 *1 subtypes (*1g, *1h, *1l, *1n to *1s, *1u, *1v, and other very rare 17 haplotypes), and eight haplotypes with nonsynonymous variations (*5b, *6b, *7b, *9b, *10b, *12b, *13b, and *14b). The *1 subtypes inferred in only one patient are grouped into 'others' in Fig. 2, and haplotypes with nonsynonymous variations are described with '?' except for unambiguous *8b, since the predictability for these very rare haplotypes is known to be low in some cases. Overall, 49 haplotypes were determined and/or inferred. The most frequent haplotype was *1d (frequency: 0.366), followed by *1e (0.289), *1f (0.113), and *1B (0.085). Frequencies of the other haplotypes were less than 0.05.

Next, we performed network analysis using haplotypes found in more than two patients to clarify the relationships among the haplotypes. The results showed that the *1 subtypes could be further classified into six groups, *1A, *1B, *1D, *1E, *1G, and *1J groups (Fig. 3). The grouping of *1 subtypes was also shown in Fig. 2. Their frequencies were 0.435 (*1E group), 0.381 (*1D), 0.103 (*1B), 0.030 (*1G), 0.021 (*1A), and 0.013 (*1J). Five rare unclassified *1 subtypes were shown in '*1 others'. Haplotypes *5b and *6b were shown to be derived from *1d and *1B, respectively.

### Effects of CYP2C8 haplotypes on PTX metabolism

CYP2C8 catalyzes biotransformation of PTX into 6α-OH-PTX and of 3'-p-OH-PTX into diOH-PTX. The effects of *CYP2C8* haplotypes on PTX clearance, AUCs of PTX

Table 2  Summary of CYP2C8 variations detected in a Japanese population

| This study | NCBI (dbSNP) | JSNP | Reference | Location | Position NT_030059.12 | From the translational initiation site or from the nearest exon | Nucleotide change and flanking sequences (5' to 3') | Amino acid change | Allele name | Wild-type | Hetero-zygotes | Homo-zygotes | Frequency |
|---|---|---|---|---|---|---|---|---|---|---|---|---|---|
| MPJ6_2C8029a | | | | 5'-flanking | 15578352_15578350 | -667_-665b | ATAATGTAATAATAA/-CACAAATATTAT | | | 435 | 2 | 0 | 0.002 |
| MPJ6_2C8030 | rs7912549 | | [4] | 5'-flanking | 15578096 | -411b | ACATTTTTATAT/CACAAAATATAGA | | | 152 | 218 | 67 | 0.403 |
| MPJ6_2C8031 | rs17110453 | | [6] | 5'-flanking | 15578055 | -370b | CAAGGTCATAAAT/GTCCCAACTGGTC | | *1C | 201 | 184 | 52 | 0.330 |
| MPJ6_2C8023 | rs7909236 | | [6] | 5'-flanking | 15577956 | -271b | AGCACATTGGAAC/AAACCAGGGACTT | | *1B | 352 | 77 | 8 | 0.106 |
| MPJ6_2C8032a | | | | Intron 1 | 15576171 | IVS1-197 | CTGGGTCATTGCG/ATGGCACATCACA | | | 436 | 1 | 0 | 0.001 |
| MPJ6_2C8014 | | | [7] | Intron 1 | 15576095 | IVS1-121 | ATTCAGAAATATC/TGAATCTATGTGT | | | 436 | 1 | 0 | 0.001 |
| MPJ6_2C8010 | rs2275622 | IMS-JST071855 | [4] | Intron 2 | 15575704 | IVS2-64 | TGCATGGCTGCCA/GAGTGTTGCAGCA | | | 120 | 212 | 105 | 0.483 |
| MPJ6_2C8001 | rs11572078 | IMS-JST077576 | [4] | Intron 2 | 15575653_15575652 | IVS2-13_-12 | AGTTTCTGCCCC-/TTTTTTTATAG | | | 142 | 205 | 90 | 0.441 |
| MPJ6_2C8015 | | | [7] | Exon 3 | 15575497 | 475b | GAGTTGAGAAAAA/-CCAAGGGTGGGT | 159fsX18 | *5 | 435 | 2 | 0 | 0.002 |
| MPJ6_2C8019 | rs3752988 | | | Intron 3 | 15573409 | IVS3-166 | AACTCATATTTAA/GGGTAAAAGTAAT | | | 141 | 207 | 89 | 0.441 |
| MPJ6_2C8016 | rs11572091 | IMS-JST105874 | | Intron 3 | 15573340 | IVS3-97 | TTTGTAAGGATATT/-GTTAAAATTTC | | | 427 | 9 | 1 | 0.013 |
| MPJ6_2C8033a | | | [7] | Intron 3 | 15573264_15573263 | IVS3-21_-20 | AATAATTTTTT/-TAAAAATTTTAA | | | 436 | 0 | 0 | 0.002 |
| MPJ6_2C8004 | rs7098376 | | [5] | Intron 3 | 15573214 | IVS3-21 | TAATAATTTTTT/AAAAAATTTTAA | | | 409 | 28 | 0 | 0.032 |
| MPJ6_2C8034 | | | [8] | Exon 4 | 15573169 | 511b | ACTTTCATCCTGG/AGCGTGTGCTCCCT | Gly171Ser | *6 | 435 | 2 | 0 | 0.002 |
| MPJ6_2C8035 | | | [8] | Exon 4 | 15573169 | 556b | GTTTTCCAGAAAC/TGATTTGATTATA | Arg186X | *7 | 436 | 1 | 0 | 0.001 |
| MPJ6_2C8036 | | | [8] | Exon 4 | 15573169 | 556b | GTTTTCCAGAAAC/GGATTTGATTATA | Arg186Gly | *8 | 436 | 1 | 0 | 0.001 |
| MPJ6_2C8037a | rs11572093 | | [4] | Intron 4 | 15573039 | IVS4+44 | CATTTATTCAAGG/TTTGTAGGGAAGA | | | 436 | 1 | 0 | 0.001 |
| MPJ6_2C8024 | | | | Intron 4 | 15572932 | IVS4+151 | CTTTGATTTCCTG/AATTCAAAATTTTC | | | 411 | 26 | 0 | 0.030 |
| MPJ6_2C8038a | | | | Intron 4 | 15567024 | IVS4-230 | GACGAGTTATTGG/AGTGCAGTACACC | | | 436 | 1 | 0 | 0.001 |
| MPJ6_2C8039a | | | | Intron 4 | 15567008 | IVS4-214 | CAGTACCACCAACC/ATGGCACATGTAT | | | 436 | 1 | 0 | 0.001 |
| MPJ6_2C8020 | rs1926705 | | | Intron 4 | 15566944 | IVS4-150 | AGAACTTAAAGTG/ATAATAAAAAATG | | | 119 | 214 | 104 | 0.483 |
| MPJ6_2C8025a | | | | Intron 4 | 15566937 | IVS4-143 | AAAGTGTAATAAA/GAAATGTATATAT | | | 436 | 1 | 0 | 0.001 |
| MPJ6_2C8012 | rs11572101 | | | Intron 4 | 15566888 | IVS4-94 | GACATGATGTCTT/CATTCATATTTAT | | | 141 | 207 | 89 | 0.441 |
| MPJ6_2C8040 | | | [9] | Exon 5 | 15566768 | 669b | CCCTCTACTCATT/GGATTGTTTCCCA | Ile223Met | *13 | 436 | 1 | 0 | 0.001 |
| MPJ6_2C8041 | | | [9] | Exon 5 | 15566725 | 712b | CTTAAAAATGTTG/CCTCTTACACGAA | Ala238Pro | *14 | 436 | 1 | 0 | 0.001 |
| MPJ6_2C8026 | | | [8] | Exon 5 | 15566697 | 740b | ACATTAGGGAGAA/GAGTAAAAGAAACA | Lys247Arg | *9 | 436 | 1 | 0 | 0.001 |
| MPJ6_2C8027a | | | | Intron 5 | 15566597 | IVS5+21 | TTAGCAACAGATC/TAGTATTTTGATT | | | 435 | 2 | 0 | 0.002 |
| MPJ6_2C8042a | | | | Intron 6 | 15553909 | IVS6+184 | GGAGGAGGATGAC/GAGAGATCAGTAG | | | 433 | 4 | 0 | 0.005 |
| MPJ6_2C8021 | rs1891071 | IMS-JST082397 | | Intron 6 | 15553897 | IVS6+196 | CAGAGATCAGTAG/AAAACAGTATGGC | | | 124 | 215 | 98 | 0.470 |
| MPJ6_2C8043a | | | | Intron 6 | 15553794 | IVS6+299 | ATTGCCCTAGTAT/CTGAATGTTGGTT | | | 436 | 1 | 0 | 0.001 |
| MPJ6_2C8044 | | | [8] | Exon 7 | 15551173 | 1149b | CCTCATCCCCAAG/TGTAAGCTTGTTT | Lys383Asn | *10 | 436 | 1 | 0 | 0.001 |
| MPJ6_2C8013 | rs2275620 | IMS-JST071852 | [4] | Intron 7 | 15551124 | IVS7+49 | CTGAAATTTCCAT/AAGTGCTGGTTTG | | | 124 | 215 | 98 | 0.470 |
| MPJ6_2C8017 | | | [7] | Intron 7 | 15551102 | IVS7+71 | TTGGTTCCAACCC/TTCTAACAACACA | | | 430 | 7 | 0 | 0.008 |
| MPJ6_2C8007 | | | [5] | Exon 8 | 15547241 | 1230b | CTTTGACCCTGGC/TCACTTTCTAGAT | Gly410Gly | | 424 | 13 | 0 | 0.015 |
| MPJ6_2C8008 | rs1934951 | IMS-JST071853 | [5] | Intron 8 | 15547074 | IVS8+106 | GAATTGCTATTTG/ATCCATGATCAAG | | | 143 | 201 | 93 | 0.443 |
| MPJ6_2C8022 | rs2275621 | IMS-JST071854 | | Intron 8 | 15547050 | IVS8+130 | GAGCACCACTCTT/CAACACCCATGTG | | | 430 | 7 | 0 | 0.008 |
| MPJ6_2C8018 | rs11572177 | | [7] | Intron 8 | 15545796 | IVS8-204 | GATAGCAAATATA/GTCTCTTTTGTA | | | 403 | 33 | 0 | 0.040 |
| MPJ6_2C8045 | rs3832694 | IMS-JST091412 | | Exon 9 | 15545502_15545500 | 1382_1384b | ACCTGAAATCTGTTG/-ATGATTAAAGA | del 461Val | *12 | 436 | 1 | 0 | 0.001 |
| MPJ6_2C8009 | rs1058932 | IMS-JST091413 | [5] | 3'-UTR | 15545387 | 1497b(*24)c | CCATCTGCGTGCC/TGATCTGCTATCA | | | 143 | 196 | 98 | 0.449 |
| MPJ6_2C8046a | | | | 3'-UTR | 15545208 | 1676b(**203)c | ACTCTGTAAACACT/-TGTATTAATTGC | | | 434 | 3 | 0 | 0.003 |

aNovel variations detected in our study.
bA of the translation initiation codon ATG is numbered +1.
cThe nucleotide number from the end of translational termination codon.
SNP, single nucleotide polymorphism.

**Fig. 1**
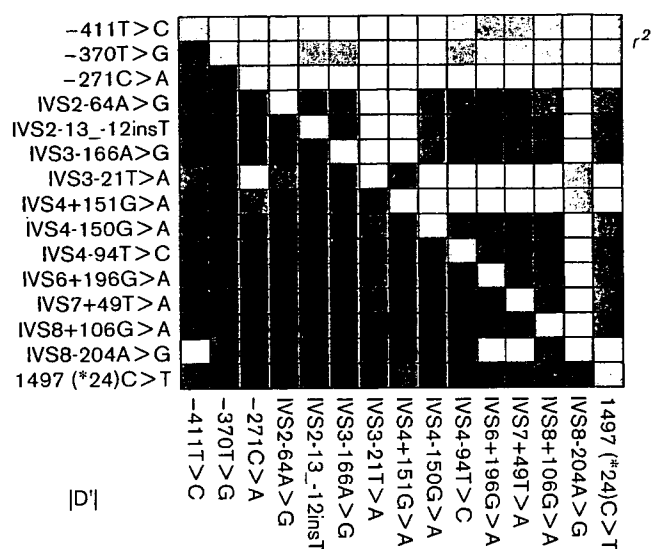


Linkage disequilibrium (LD) analysis of *CYP2C8*. Pairwise LD between variations with ≥ 3% frequencies is expressed as |D'| (lower left) and $r^2$ (upper right) by 10-graded blue colors. A denser color represents a higher linkage.

and its metabolites, and metabolic ratios (ratios of metabolite AUCs to PTX AUC) were investigated in 199 PTX-administered patients.

Because nonsynonymous variations were all rare, we focused on the effects of diplotypes using grouped *1 haplotypes (i.e. *1A, *1B, etc). No significant differences were observed in clearance of PTX, AUCs of PTX, 6α-OH-PTX and diOH-PTX, and AUC ratio of 6α-OH-PTX/ PTX among the grouped *1-diplotypes found in more than three patients (data not shown). A statistically significant deviation, however, was observed in AUC of 3'-p-OH-PTX among the grouped *1-diplotypes ($n ≥ 3$) ($P = 0.014$ by Kruskal–Wallis test) (Fig. 4a). Furthermore, AUC ratio of 3'-p-OH-PTX/PTX also showed a tendency to be different among the grouped *1-diplotypes of $n ≥ 3$ by the same test ($P = 0.071$) (Fig. 4b). Careful analysis revealed that significant differences in both parameters were observed between *1D/*1D and *1G/*1D patients ($P < 0.05$ for both parameters, Mann–Whitney $U$-test) and between *1E/*1E and *1G/*1E patients ($P < 0.001$ for AUC of 3'-p-OH-PTX and $P < 0.01$ for AUC ratio of 3'-p-OH-PTX/PTX) (Fig. 4).

Next, heterozygous *1G diplotypes were combined into *1G/non-*1G diplotypes ($n = 11$). Because no significant differences were observed among the other *1/*1 groups, all the other *1/*1 diplotypes were combined into one group, designated as non-*1G/non-*1G. As shown in Fig. 5a, the median AUC of 3'-p-OH-PTX was about 2.5-fold

higher in the *1G/non-*1G patients than in the non-*1G/ non-*1G patients ($P < 0.001$ by Mann–Whitney $U$-test). The median value of 3'-p-OH-PTX/PTX AUC ratio was also about 64% higher in the *1G/non-*1G patients than in the non-*1G/non-*1G patients ($P < 0.001$, Fig. 5b). In contrast, there were no significant differences in AUC of 6α-OH-PTX and AUC ratio of 6α-OH-PTX/PTX between the two groups (Fig. 5c and d) although the AUC ratio was about 9% lower in the *1G/non-*1G patients than in the non-*1G/non-*1G patients (Fig. 5d). Considering the metabolic route of PTX, these findings suggest that CYP2C8 activity is probably reduced in the *1G-bearing patients.

Recently, we have shown that *CYP3A4*16B* (and probably *6, $n = 1$) decreases the AUC ratio of 3'-p-OH-PTX/PTX, and that no other major *CYP3A4* haplotypes significantly affect the AUC ratio and other PK parameters analyzed [9]. Therefore, we analyzed the effects of *1G on the AUC of 3'-p-OH-PTX and AUC ratio of 3'-p-OH-PTX/ PTX excluding *CYP3A4*16B*- and *6-bearing patients and confirmed the increasing effects of *1G ($P < 0.001$ for both by Mann–Whitney $U$-test). In addition, the significantly increasing effects of *CYP2C8*1G* were also observed within *CYP3A4*1A/*1A* patients ($P < 0.001$ for AUC of 3'-p-OH-PTX and $P < 0.01$ for AUC ratio of 3'-p-OH-PTX/PTX, Mann–Whitney $U$-test). Furthermore, distributions of *CYP3A4* diplotypes/haplotypes were not significantly different between the *CYP2C8*1G/non-*1G* patients and the non-*1G/non-*1G patients ($P > 0.05$ by Fisher's exact test). These results suggest that the effects of *CYP2C8*1G* are independent of the *CYP3A4* genotypes. Gender also affects the AUC ratio of 3'-p-OH-PTX/PTX [9]. Statistical analysis using data from men only also gave almost the same increasing effects of *1G ($P < 0.001$ for the AUC of 3'-p-OH-PTX and $P = 0.001$ for the AUC ratio of 3'-p-OH-PTX/PTX, Mann–Whitney $U$-test).

To identify further the genetic variation responsible for the increased AUC of 3'-p-OH-PTX and increased AUC ratio of 3'-p-OH-PTX/PTX, we next focused on the variations in the *1G group. Among them, the patients bearing IVS3-21T > A showed statistically significant increases in these parameters compared with the patients without this variation ($P < 0.001$ for both parameters, Mann–Whitney $U$-test). The *1t haplotype also harbored IVS3-21T > A, and one patient with the *1t/*1d diplotype (grouped into *1D/*1D) had the second highest AUC of 3'-p-OH-PTX (1.07 h*μg/ml) and the second highest AUC ratio of 3'-p-OH-PTX/PTX (0.0497) in the 24 *1D/*1D patients (Fig. 4, grey arrowheads). These findings suggest that IVS3-21T > A might be involved in the altered CYP2C8 activity, although we cannot exclude the possibility that other identified/unidentified linked variation is causative.

**Fig. 2**



Haplotype structures of *CYP2C8* in Japanese population. Haplotypes are described with numbers plus alphabetical letters, and the *1 haplotypes (without amino-acid change) were grouped based on network analysis (Fig. 3). Because rare *1 haplotypes found in only one individual were grouped into 'others', the seven variations detected only in the rare haplotypes (IVS1 −197G>A, IVS1 −121C>T, IVS4+44G>T, IVS4−230G>A, IVS4−214C>A, IVS4−143A>G, and IVS6+299T>C) are not shown in this figure. Numbers in parenthesis in the 'Number' section indicate patient numbers used for association analysis for pharmacokinetic parameters of PTX. White, major allele; yellow with a haplotype name, minor allele; yellow without a haplotype name in 'others', common variations of the 'others' group. In yellow with a haplotype name, nonsynonymous variations are shown by a red number.